Geo-Marine Letters (2019) 39:313–336
https://doi.org/10.1007/s00367-019-00576-0

ORIGINAL

Ostracods and mollusks in northern Sfax coast: reconstruction of Holocene paleoenvironmental changes and associated forcing

Afef Khadraoui[1] · Chahira Zaïbi[1] · Pierre Carbonel[2] · Jérôme Bonnin[2] · Fekri Kamoun[1]

Received: 26 June 2018 / Accepted: 29 May 2019 / Published online: 20 June 2019
© Springer-Verlag GmbH Germany, part of Springer Nature 2019

Abstract

The present study investigates the history of the northern Sfax coast by means of subsurface sediments of the sebkhas El Merdessia and El Awebed through a multiproxy approach. Ostracod and mollusk assemblages, diversity index, sedimentological criteria, correspondence analysis, and radiocarbon datings together provide an overview of the development of this coast over the last 5000 years. Original data give evidence for periods of predominantly lagoonal and brackish water conditions. These data testify to the emersion of sebkha El Awebed during Holocene, while sebkha El Merdessia recorded three marine transgressions toward 4599, 2225, and 1396 years cal BP. These transgressions are indicated by the richness of sediments in lagoonal and marine ostracod assemblages coupled with marine mollusks and the high values of species richness and diversity index. Sandwiched between 2225 and 1396 years BP, a period of sea-level stability and buildup of sand barriers in front of the estuaries was evidenced. Toward 250 years cal BP, a tsunami event is evidenced by the deposition of a shelly bed containing angular and sharpened *Cerithium vulgatum* in coarser marine sands overlaid by silts and clays rich in charcoal particles and pottery fragments. The comparison between the proxies analyzed of the studied area and those of Skhira coast leads to the conclusion that the two coasts were subjected to the same factors. However, a time shift of sedimentation is due to the uplift of Sfax northern coast favored by the activity of the faults, unlike the southern Skhira subsidence.

Introduction

Enclosed by a calcite carapace made up of two valves, which are easy to fossilize, ostracods are indicators of the bathymetry, the hydrodynamic conditions, and the nature of substratum of marine, lagoonal, and estuarine environments. Carbonel (1988) and Boomer and Eisenhauer (2002) remark that microfauna density, species richness, and diversity index are influenced by environmental conditions. Also, ostracods are good bioindicators of sea-level variation (Milker et al. 2012), water depth (Frenzel et al. 2010), water quality (Padmanabha and Belagali 2008), and marine invasion on the continent (Baumann et al. 2017). Their valve morphology, surface reticulation, thickness, carapace size, and sieve pore shape are useful to identify dissolved oxygen concentration (Carbonel 1988; Boomer and Whatley 1992) and different types of environments (Peypouquet et al. 1988). Due to their rapid response to environmental disturbances, the ostracods characterize short deposit environments over time and very shallow water depths. The differentiation between allochthonous and autochthonous valves and shallow water species from deep-water taxa could reflect different types of sediment transport processes (Carbonel and Jouanneau 1982). Recently, ostracods have been used to recognize extreme events such as storms and tsunamis. Abrantes et al. (2005), Ruiz et al. (2007), Zaïbi et al. (2016), and Khadraoui et al. (2018) discussed the impact of these events on environmental change. The paleontological criteria of tsunami deposits were found to be as follows: (i) deposits may contain mollusk shells of a wide range of habitats in low to high concentrations, largely depending on sediment source (Donato et al. 2008; Richmond et al. 2012; Engel et al. 2016); (ii) large shells are often found convex-up (Reinhardt et al. 2006; Engel et al. 2016; Bernabéu-Puga and Aguirre 2017); (iii) tests may be crushed/broken in significant percentages and an allochthonous mixing of articulated

Electronic supplementary material The online version of this article (https://doi.org/10.1007/s00367-019-00576-0) contains supplementary material, which is available to authorized users.

✉ Afef Khadraoui
afefkhadraoui1988@gmail.com

[1] GEOGLOB Laboratory, Faculty of Sciences of Sfax, Sfax University, BP 1171, 3000 Sfax, Tunisia

[2] EPOC, UMR 5805, Bordeaux University, Allée Geoffroy Saint-Hilaire, 33615 Pessac cedex, France

Bivalvia species out of life position; (iv) foraminifera and ostracod assemblages are diverse and include a variety of predominantly marine species (Hindson et al. 1996; Hindson and Andrade 1998); and (v) adult/juvenile ostracod ratios usually change compared to vertically confining background sediments.

Several studies have been realized in Tunisia on ostracods from Ichkeul Lake fresh/saline waters (Stevenson et al. 1993; Ben Hamad et al. 2018), Tunis lake marine/lagoonal water (Carbonel and Pujos 1981; Carbonel 1982), and Ghar el Melh, Ariana, and Soliman sebkha lagoonal/brackish waters (Mansouri-Menaouar et al. 1979; Mansouri-Menaouar and Carbonel 1980; Ruiz et al. 2006). These authors have identified, through the ostracod taxa, numerous associations characterizing the evolution of Holocene environments.

Our previously realized works on the Gulf of Gabes concerned the southern Skhira and the northern Sfax coasts. In fact, Zaïbi et al. (2011, 2012, 2016) identified the evolution of the Skhira coast during Holocene times, by means of Ostracoda, foraminifera, and mollusk associations and recognized seven categories of lagoons, sebkha, and transgressive biofacies and their geochronological respective ages. Also, two peculiar biofacies, formed by coarse sands or shelly clays showing a mixture of lagoonal, marine, and brackish taxa of mollusk, provide evidence of high-energy events. Khadraoui et al. (2018), for El Merdessia sebkha situated at northern Sfax coast, reconstructed the paleoenvironments during upper Holocene, recognized the period of alongshore drifts during sea-level stability, identified three transgressive episodes, and characterized, for the first time, a tsunami event and its micropaleontological and sedimentological criteria.

Following on from our preliminary results (Zaïbi et al. 2016; Khadraoui et al. 2018), the present work investigates the two sebkhas of El Awebed and El Merdessia in the northern Sfax coast and aims at (1) reconstructing the different paleoenvironments, and their respective biofacies, which succeeded during the Holocene time, and discussing the factors controlling paleoenvironmental changes; (2) describing and comparing the morphological evolution of Sfax and Skhira coasts; and (3) scrutinizing and comparing the mechanisms of their evolution then providing future evolution scenarios within a global context. These objectives require ostracod and mollusk studies, along with the analysis of the geomorphologic and hydrodynamic settings and recent evolutionary trends.

Study area

The studied area corresponds to the northern part of the Gulf of Gabes (Fig. 1a). The latter consists of a relatively plane domain characterized by the presence of coastal lagoons (Mahras, El Hisha, Boughrara, El Biban), sebkhas (Ouadrane, El Guettiate, Dreiia, Boujmel), and estuaries/delta (Gargour, Ouadrane, El Akarit) along the coastline (Fig. 1b). These lagoons and sebkhas have been isolated, since the Holocene time, from the open sea by a sandy spit system (Zaïbi et al. 2016), eolian littoral dunes, and a carbonate sand beach (Jedoui 2000). This configuration seems to be the result of Quaternary transgressive tectonic events generating horsts and small grabens (Perthuisot 1975) and sedimentary dynamics (Zaïbi et al. 2012). Among these depressions, the studied sebkhas El Merdessia and El Awebed are visible in the northern coast of Sfax over a surface of about 6 km^2 (Fig. 1c). This area, characterized by a regular topography, is confined between Sidi Mansour Cape to the south and El Awebed Harbor to the north. Currently, it is a small modern coastal tidal system characterized by a warm and arid climate, with annual rainfall of only about 300 mm. Both sebkhas are episodically supplied by seawater during the exceptional tides and storms. The amplitude of the semidiurnal tides ranges from 80 to 150 cm. It plays an important role as it determines a peritidal system showing three different zones arranged from west to east as follows: (i) *a land* characterized by the presence of several archeological sites and developed vegetation with a succession, from east to west, of Salicornia and olive plantations. The morphostructural map of this area reveals the presence of corridors of N 120–140 faults (Houla et al. 2013) which control the deviation of an intermittent streams course, locally called Làachech wadi. The latter flows in El Merdessia and El Awebed sebkhas; (ii) *a supratidal zone*, which corresponds to the two sebkhas and extends over 800 m landwards. As the surface sediments of the sebkhas are constituted of yellow clays rich in salt crystals, the substratum is composed of white quartz sands rich in mollusks, Upper Pleistocene in age, corresponding to the marine isotopic stage (MIS 5.5). These quartz sands outcrop along the coastline and give rich assemblage constituted by *Glycymeris violascescens*, *Cerithium vulgatum*, *Cerastoderma glaucum*, *Dentalium* sp., and the Senegalese taxa *Persististrombus latus*. The latter is a tropical water organism that colonized the Mediterranean Sea during the last interglacial and an important stratigraphic marker of marine isotope stage (MIS 5.5); (iii) *an intertidal zone* exhibiting several small gulfs colonized by tight halophile vegetation, such as *Salicornia* sp. The developed slikkes, flooded at high tide, are made up of silty sands. The intertidal zone extending about 300 m in front of El Awebed sebkha is further developed to the south and reaches 1 km. Several Roman ruins stand along Sfax coastline, some of which are submerged by the sea waves. Along this coast, the levels at *Persististrombus latus* are visible and submitted to the action of waves. The intertidal mudflats provide habitat for birds during winter, and (iv) *a subtidal zone* constantly flooded and characterized by shallow water. The isobath 20 m is at 5 km from the coastline. The subtidal mudflat substratum is rich in phanerogams, mainly *Posidonia* and *Cymodocea*.

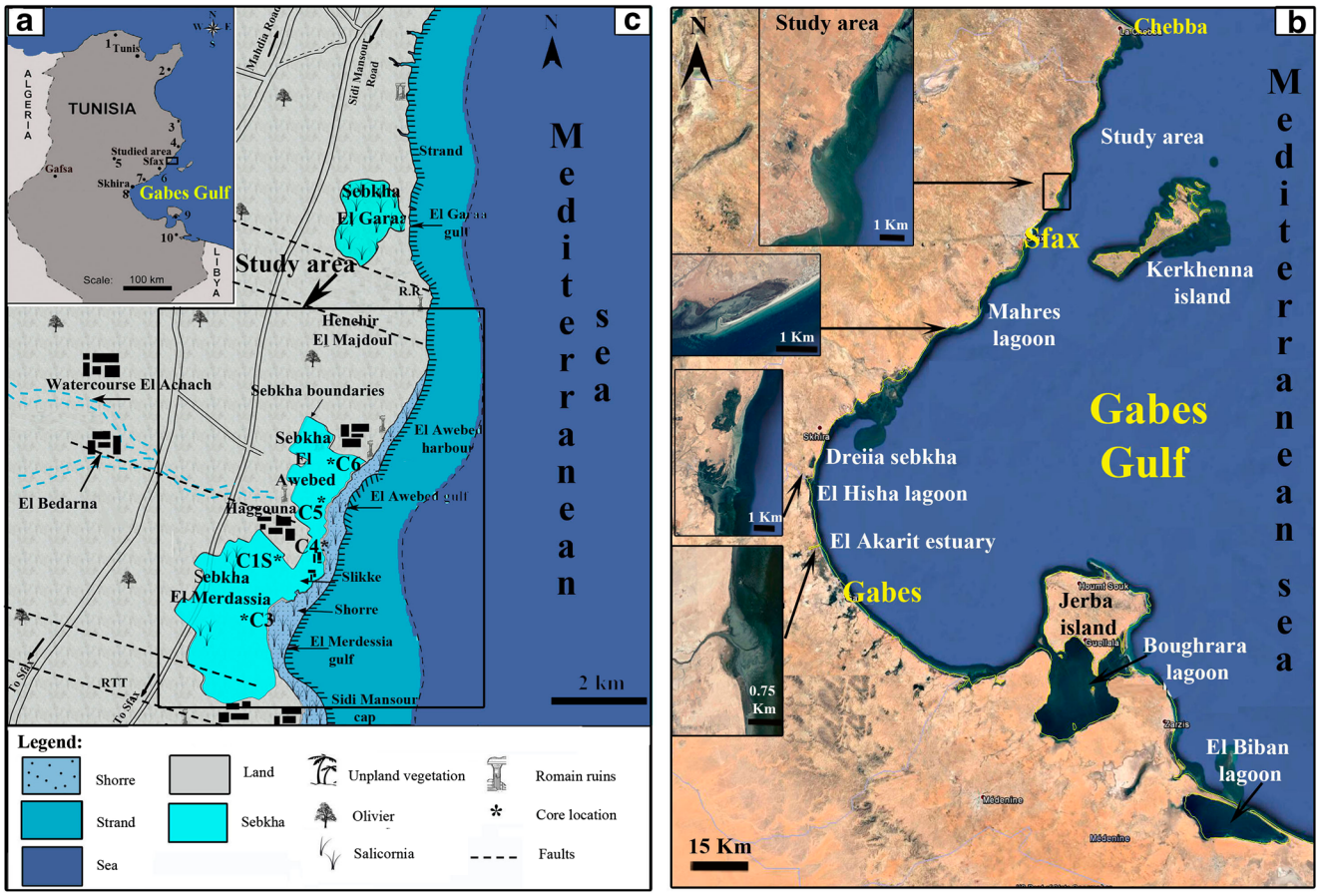

Fig. 1 **a** Location map of the studied area and positions of localities cited in the text. 1: Ichkeul Lake, 2: Cap Bon, 3: Rass Dimass, 4: Ras Botria, 5: Makanassy area, 6: Gargour Coast, 7: Aouled Ridha Sebkha, 8: Dreiia Sebkha, 9: Jerba Island, 10: Boujmal Sebkha. **b** Detailed view of paralic environment of Gulf of Gabes coast cited in the text and position of the study area. **c** Location of El Merdessia and El Awebed Sebkhas, distribution of different littoral environments, geomorphological units, and positions of cores

Materials and methods

Fieldwork and sampling

To reconstruct the development of the two sebkhas El Merdessia and El Awebed, five sediment cores C1S, C3, C4, C5, and C6 were collected from boreholes drilled in the area of sebkhas at about 0.5 m above sea level (Table 1). In addition, many lithologic cross sections, of coastal outcrops and trenches, were characterized by surface measurements, sampling, and detailed facies descriptions. The sampling interval is about 5 cm where principal shoreline features are positioned in the cross-shore profile. The coring method consists in introducing by manually knocking a PVC tube of 50 mm in diameter. In the laboratory, the cores were divided into two halves, lengthwise. One half was photographed, described (type, color, structure, and organic content of the sediment), and sampled at each centimeter for C1S and C3 cores, each 5 cm for C4 and each 2 cm for C5 and C6 cores. The obtained samples were dried and weighed. They were used for grain size distribution and macro- and microfauna analyses. For paleontological analyses, each sample was washed over 63 and 125 μm sieves and different weight fractions (< 63, 63–125, and > 125 μm) were separated.

Table 1 Location of El Merdessia and El Awebed cores (C3, C4, C1S, C5, and C6)

Cores	Location
C1S	34° 50′ 16.44″ N–10° 52′ 7.71″ E
C3	34° 49′ 55.06″ N–10° 52′ 3.81″ E
C4	34° 50′ 47.15″ N–10° 53′ 11.85″ E
C5	34° 51′ 10.10″ N–10° 53′ 16.30″ E
C6	34° 51′ 32.68″ N–10° 53′ 38.01″ E

Ostracod and mollusk identification and statistical analyses

The residue of each sample was poured through a microsplitter and divided into several aliquots. All specimens of microfauna, contained in one aliquot, were hand-picked using a wet brush. If less than 300 specimens were present

per aliquot, another aliquot of sediment was picked. This number guarantees a representative population for the high diversity assemblages (Fatela and Taborda 2002). Ostracod specimens were identified, counted, and standardized to 10 g dry sediment for each sample. The taxonomical keys were provided by Bonaduce et al. (1975), Athersuch et al. (1989), and Zaïbi et al. (2012) for ostracods and by Bouchet and Rocroi (2005, 2010) for Gastropoda and Bivalvia. The selected parameters were density (number of individuals), species richness, Shannon–Wiener index (*H*) used to characterize species diversity in the community, and equitability index (*E*) of Pielou (1966). All these parameters were calculated using PAST software (Hammer et al. 2001). Paleoenvironmental interpretation of ostracod and mollusk assemblages was based on data from the Mediterranean lagoonal system that includes both modern and Holocene information on mollusk and Ostracod distribution and abundances (Carbonel 1988; Mansouri-Menaouar and Carbonel 1980; Ruiz et al. 2005; Trog et al. 2013; Zaïbi et al. 2016). A selection of ostracod species was photographed as shown in Plate 1. A correspondence analysis (CA), performed on both ostracod and mollusk data (assemblages, density, species number, taxa, and mollusk fragments) and samples, was carried out to clarify the micropaleontological results. The minimum of occurrence of taxa included in the matrix is 4%.

Radiocarbon dating and age model

For radiocarbon dating, well-preserved Bivalvia and Gastropoda shells were considered to be the main control for core lithological units. The ^{14}C datings were carried out at the laboratories of Climate and Environment of CNRS (Gif-sur-Yvette, France), the Isotopic and Palaeoclimatology Laboratory at the National School of Engineers (E.N.I.S, Sfax, Tunisia), and Mesure du C14 (ARTEMIS) (Saclay, France). All samples were prepared following a standard procedure (Delibrias 1985). Results of radiocarbon dating are presented as conventional ^{14}C ages and calibrated dates, calculated using the CALIB radiocarbon calibration software (version 7.10, Stuiver and Reimer 1993). Depending on the $\delta^{13}C$ values, each sample was calibrated using MARINE13 calibration curves (Reimer et al. 2013). The calibrated dates were corrected for marine reservoir effects using delta *R* correction of 35 ± 70 years as proposed by Siani et al. (2000) for the modern period and Siani et al. (2001) for the last 6000 years in the Mediterranean Sea. The ages discussed below are expressed as median age (Table 2). We also integrated in this table the C14 dating results of the cores C2, CD2, SG1, CII, and BSC2 of our previous works (Zaïbi et al. 2016) herein recalibrated. The age model developed for the cores of southern Skhira (Zaïbi et al. 2016) and of northern Sfax coasts, based in radiocarbon age, was established assuming that the sedimentation rates were constant between each of the dates obtained through radiometric dating (Fig. 2). In fact, the estimated sedimentation rate in southern Skhira coast for the interval between 7460 and 3535 years is relatively low and situated between 0.2 and 0.3 mm/year. Afterward, sedimentation rate increases to 0.5 mm/year between 3535 and 753 years. In Sfax northern coast, the sedimentation rate is comparable to that of southern Skhira and is about 0.3 mm/year between 4599 and 357 years BP. However, these sedimentation rates should be considered with caution if a major event was responsible for a sudden sediment deposition, which would likely increase the sedimentation rate presented in Fig. 2 as the case of 5 and 2 mm/year rates estimated for southern Skhira cores and interpreted as the result of a washover event (Zaïbi et al. 2016).

Results

Lithological units and radiometric dating

El Merdessia sebkha

Core C3 The core C3, 131 cm long, shows eight lithological units (Fig. 3). The lowest unit (U1, 131–100 cm below the surface) is characterized by white quartz sands, Upper Pleistocene in age, rich in bio- and lithoclasts and in lagoonal and marine mollusks in their upper part. The second unit (U2, 100–83 cm), showing a fining-upward sequence, has an erosional base and contains well-preserved Bivalvia and Gastropoda (*Hydrobia ventrosa*, *Cerithium vulgatum*) and reworked mollusks and intraclasts from U1 unit in very coarse sands. From 83 to 63 cm, (U3) is characterized by sands rich in lagoonal mollusks including unbroken (70%) and broken (30%) items. Unit U4 (63–43 cm) is made up of azoic dark silt. U5, from 43 to 35 cm, is composed of azoic gray clays. The sands rich in mollusks and phanerogams constitute U6 (35 to 20 cm). From 20 cm to the surface, azoic gray clays (U7) and silts (U8) correspond to the upper part of C3 core.

One ^{14}C dating was obtained on Bivalvia and Gastropoda shells for unit 2 (89–93 cm), indicating the age 2225 years cal BP (Table 2).

Core C1S It involves four lithological units labeled U1 to U4 (Fig. 3). Between 85 and 65 cm (U1), the core C1S is characterized by a sequence of coarse sands rich in *Hydrobia ventrosa* lagoonal gastropods and lithoclasts. The fine sediment fraction varies between 10 and 30%. The second unit (U2, 65–36 cm) has an erosional contact and is made up of coarser sands. It contains lagoonal bivalves (*Cerastoderma glaucum*, *Abra alba*), Gastropods, lithoclasts, and charcoal particles. The high content of mollusk fragments, lithoclasts, and coarse fraction, which reach up to 90%, also marks this

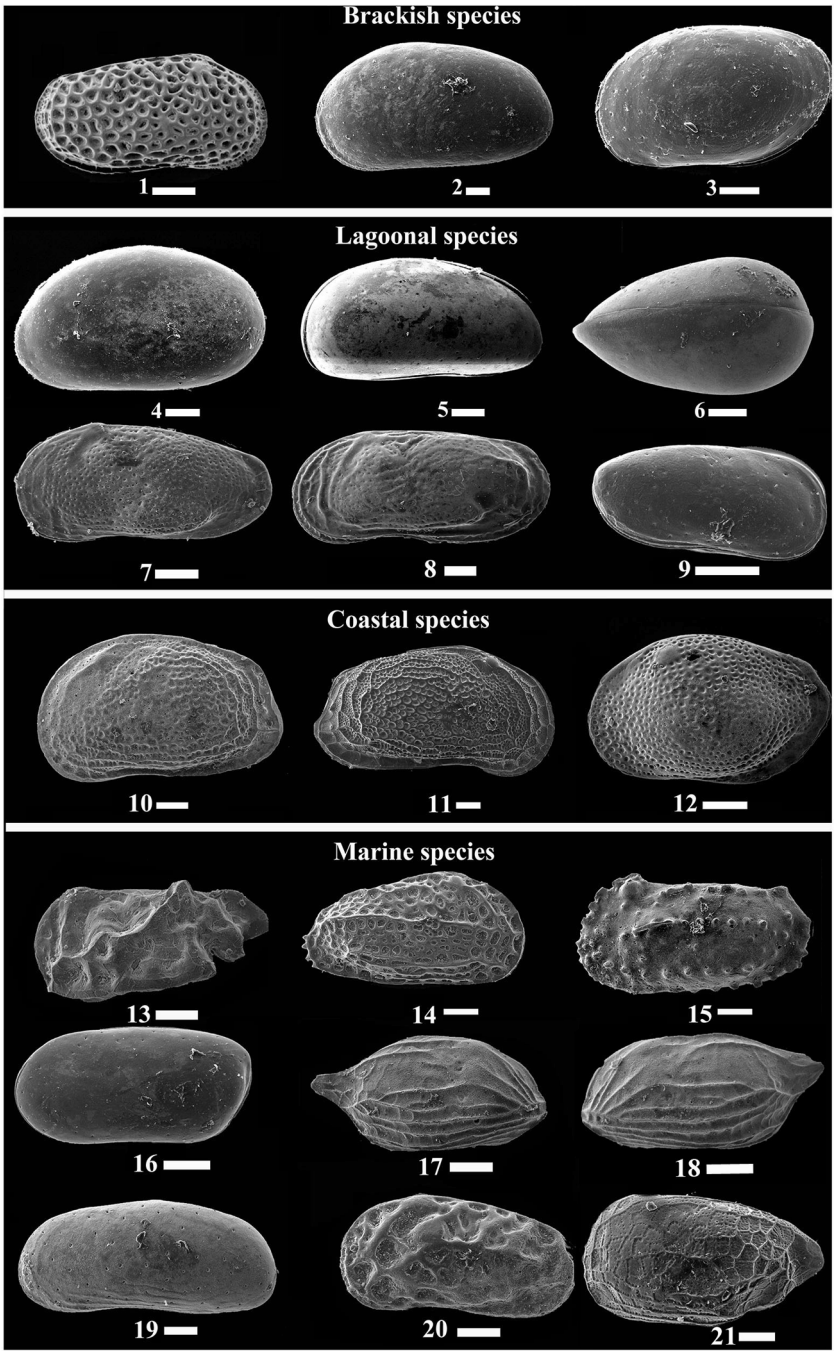

Plate 1 Ostracod shells from Sebkha of El Merdessia, cores C3, C4, and C1S. 1. *Cytheromorpha fuscata* (Brady), right valve. 2. *Cyprideis torosa* (Jones): male carapace (Cp), left valve. 3. *Loxoconcha elliptica* (Brady), left valve. 4. *Xestoleberis aurantia* (Baird), left valve. 5, 6. *Xestoleberis dispar* (Mueller); 5, right valve; 6, carapace, dorsal view. 7. *Leptocythere* sp., left valve. 8. *Leptocythere fabaeformis* (G.W. Müller), left valve. 9. *Leptocythere pellucida* (Baird), right valve. 10. *Aurila prasina* (Barbeito-Gonzalez), left valve. 11. *Aurila* sp., right valve. 12. *Loxoconcha rhomboîdea* (Fischer), left valve. 13. *Paracytheridea depressa* (G.W. Müller), left valve. 14. *Hiltermannicythere emaciata* (Brady), right valve. 15. *Carinocythereis carinata* (Roemer), left valve. 16. *Basslerites berchoni* (Brady), left valve. 17, 18. *Semicytherura incongruens* (G.W. Müller); 17, right valve; 18, left valve. 19. *Cushmanidea elongata* (Brady), left valve. 20. *Callistocythere discrepans* (G.W. Müller), left valve. 21. *Semicytherura sella* (Sars, 1866), left valve. Scale bar = 100 μm

interval. Above this unit, the sands are fine and mollusks disappear from 36 to 20 cm (U3). The last 20 cm (U4) is composed of azoic reddish silts.

Two ^{14}C datings were obtained on Bivalvia and Gastropoda, indicating the ages of U1: 1396 years cal BP (84–79 cm depth) and of U2: 250 years cal BP (57–55 cm depth) (Table 2).

Table 2 ^{14}C median ages in years cal BP obtained for the lithologic units of C1S, C3, and C4 cores of Sfax northern coast and of CII, BSC2, SG1, CD2, and C2 cores of the southern Skhira coast

Locality	Cores	Depth (cm)	Studied material	Age ^{14}C (years BP)	Calibrated age 1 sigma (years BP)	Calibrated age 2 sigma (years BP)	Median age (years BP)	Laboratory
Sebkha El Merdessia	C1S	55–57	*Cerastoderma glaucum–Cerithium vulgatum*	640 ± 168	77–399	0–502	250	Isotopic and Palaeoclimatology E.N.I.S. (Sfax, Tunisia)
	C1S	79–84	*Cerastoderma glaucum–Cerithium vulgatum*	1865 ± 169	1202–1593	1001–1804	1396	
	C3	89–93	*Cerastoderma glaucum-Cerithium vulgatum*	2595 ± 30	2139–2317	2018–2419	2225	Sciences du Climat et de l'Environnement du CNRS de Gif/Yvette
	C4	166–168	*Cerithium vulgatum*	4460 ± 30	4490–4716	4408–4802	4599	Mesure du C14 (ARTEMIS) Saclay
	C4	28–30	*Cerastoderma glaucum-Cerithium vulgatum*	745 ± 30	285–427	225–499	357	
Sebkha El-Guettiate	SG1	25–27	Gastropoda and Bivalvia	5100 ± 50	5312–5508	5235–5599	5419	Mesure du C14 (ARTEMIS) Saclay
	SG1	50–54	Gastropoda and Bivalvia	5150 ± 50	5388–5575	5286–5636	5471	Sciences du Climat et de l'Environnement du CNRS de Gif/Yvette
	SG1	109–112	Gastropoda and Bivalvia	6620 ± 40	7000–7198	6897–7271	7098	Beta Analytic, Miami, USA
	BSC2	7–17	Gastropoda and Bivalvia	6055 ± 30	6342–6525	6282–6618	6440	Sciences du Climat et de l'Environnement du CNRS de Gif/Yvette
	BSC2	38–60	Foraminifera and ostracods	6995 ± 120	7330–7576	7195–7708	7460	
	CII	21–29	Gastropoda and Bivalvia	5665 ± 30	5932–6119	5873–6212	6036	Mesure du C14 (ARTEMIS) Saclay
	CII	48–53	Gastropoda and Bivalvia	5560 ± 40	5788–6000	5708–6128	5911	Beta Analytic, Miami, USA
Sebkha Dreîaa	CD2	40	Gastropoda and Bivalvia	3110 ± 30	2756–2927	2711–3050	2856	Sciences du Climat et de l'Environnement du CNRS de Gif/Yvette
	CD2	65–70	Gastropoda and Bivalvia	3235 ± 30	2896–3112	2797–3208	3005	
	CD2	145	Gastropoda	6260 ± 40	6568–6770	6470–6872	6671	Beta Analytic, Miami, USA
	C2	201–209	Foraminifera and ostracods	3670 ± 40	3435–3635	3949–3755	3539	
	C2	59–60	Gastropoda and Bivalvia	1215 ± 30	653–797	615–902	735	Mesure du C14 (ARTEMIS) Saclay
	C2	20–37	Gastropoda and Bivalvia	1115 ± 30	562–697	516–777	644	Sciences du Climat et de l'Environnement du CNRS de Gif/Yvette

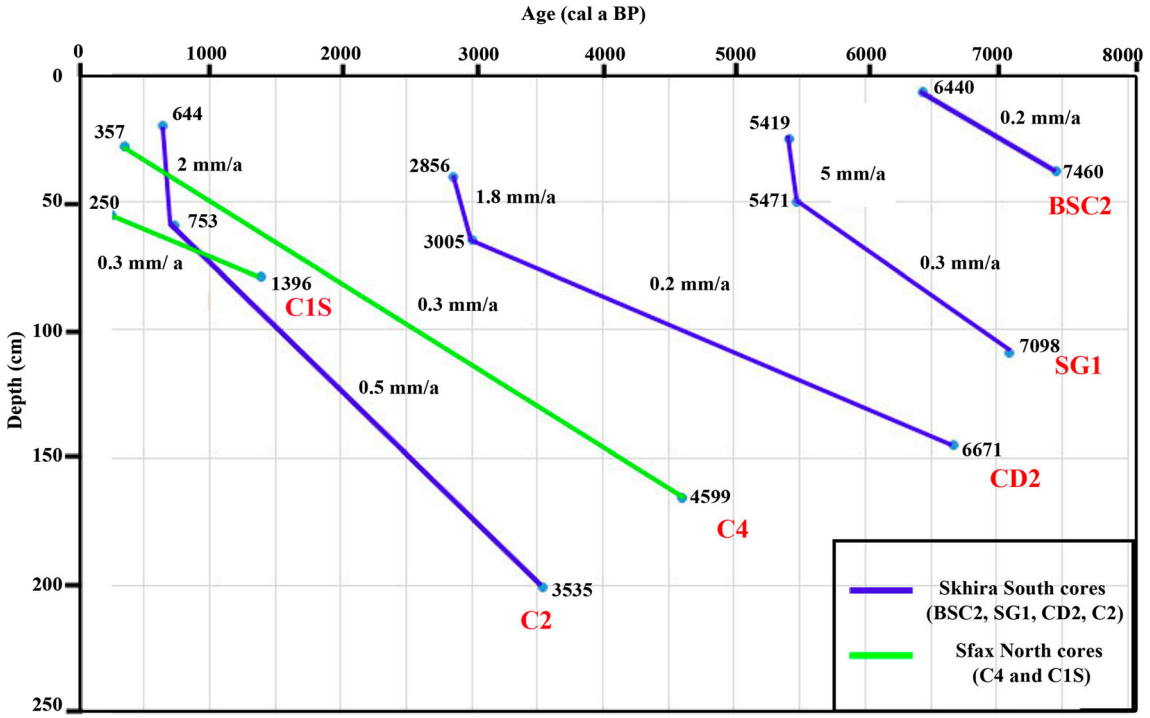

Fig. 2 Age model assuming a constant rate of deposition for the C1S, C3, and C4 cores of Sfax northern coast and of CII, BSC2, SG1, CD2, and C2 cores of the southern Skhira coast based in radiocarbon age (for details, see Table 2)

Core C4 The C4 core, 190 cm long, is divided into six lithological units (Fig. 3): The first (U1) between 190 and 157 cm consists of silts rich in mollusk fragments, lagoonal bivalvia (*Cerastoderma glaucum*, *Abra alba*) and gastropoda (*Cerithium vulgatum* and *Potamides* sp.), and marine-displaced mollusks. From 157 to 105 cm (U2), dark silty clays rich in mollusks, where the fraction < 125 μm decreases to 20%, are found. From 105 to 60 cm (U3), the sediment is built up of azoic fine sand. The unit from 60 to 30 cm (U4) is made up of an alternation of azoic silts and clays, where the fraction < 125 μm reaches up to 90%. The interval between 30 and 12 cm (U5) is marked by the presence of coarse sands characterized by a sharp erosional contact and arranged in a fining-upward sequence. These sands are rich in lagoonal and marine bivalvia and gastropoda, lithoclasts 2–4 cm in dimensions, pottery fragments, charcoal, and reworked Upper Pleistocene mollusks. Unit U6, from 12 cm to the top, is made up of silts.

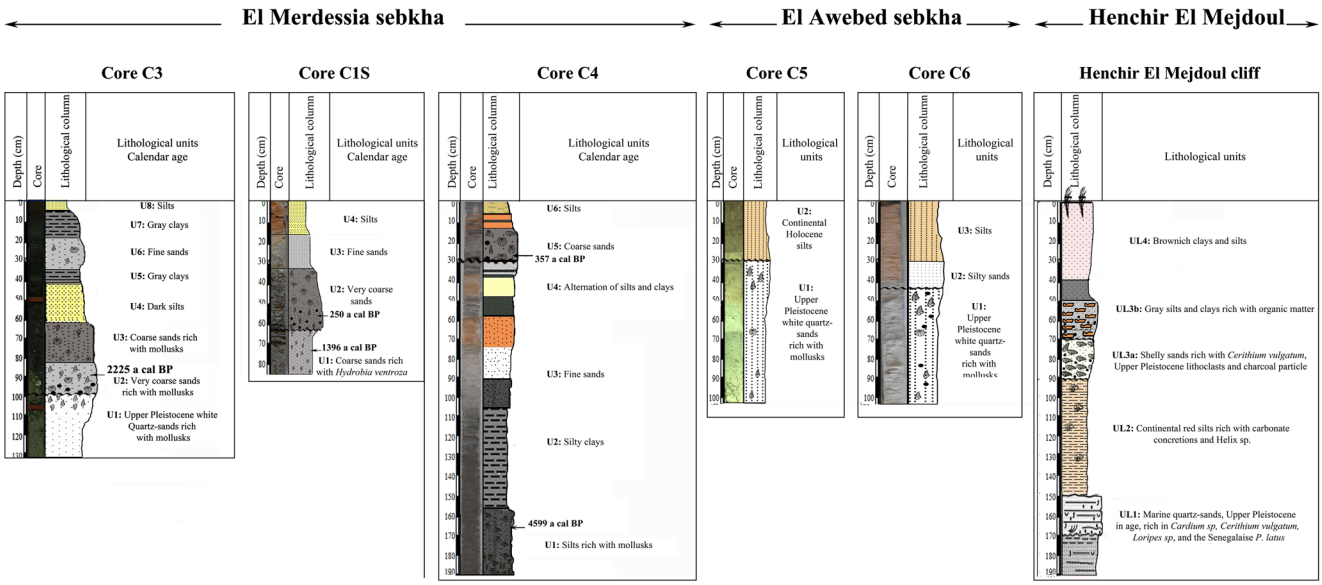

Fig. 3 Lithological units and calendar ages of C3, C4, C1S, C5, and C6 cores and Henchir El Mejdoul section

Two ^{14}C datings were obtained on Bivalvia and Gastropoda, indicating the ages of U1: 4599 years cal BP (166–168 cm depth) and of U5: 357 years cal BP (28–30 cm) (Table 1).

El Awebed sebkha

Core data

Core C5 Core C5, 100 cm in length, which bored the Upper Pleistocene substratum, is constituted by two lithological units (Fig. 3). The interval from 100 to 30 cm (U1) can be separated from the overlying one by the presence of coarse quartz sands, Upper Pleistocene in age, constituting the sebkha substratum and rich in gastropods such as the lagoonal *Cerithium vulgatum*, the warm marine taxa *Conus mediterraneus*, and the dominant lagoonal Bivalvia *Loripes* sp. associated to *Cerastoderma glaucum* and mollusk fragments. A silty interval (U2) which constitutes the last 30 cm of the core is poor in macro- and microfauna.

Core C6 Core C6 can be divided into three lithological units (Fig. 3). Coarse quartz sands, Upper Pleistocene in age, rich in *Conus mediterraneus*, characterize the lower unit (unit U1, 100–42 cm). The second unit (U2, from 42 to 32 cm) corresponds to azoic green silty sands and the last lithological unit (U3, 32 cm) is composed of silts poor in micropaleontological data and without Mollusca.

Outcrops data

The Henchir El Mejdoul cliff shows the presence of five lithological units (Fig. 3) composed from the base to the surface of: (i) marine quartz sands rich in *Cardium* sp., *Cerithium vulgatum, Loripes* sp., and conglomerates (UL1); (ii) continental red silts, 60 cm thick, rich in carbonate concretions and *Helix* sp. (UL2); (iii) shelly sands, 20 cm thick (UL3a); (iv) gray silts and clays rich in organic matter organized in fining-upward and thinning-landward sequence, 30 cm thick (UL3b); and (v) brownish clays and silts rich in pottery fragments and massive historic wall debris, 30 cm thick (UL4).

Ostracod associations

The cores, drilled in the sebkha El Merdessia, provide valuable paleontological data represented by mollusks and ostracods. The microfaunal assemblages are clearly dominated by ostracods represented by at least 21 species that belong to the dominant Cushmanideidae, Leptocytheridae, and Cytheruridеidae families. Four assemblages are recognized:

Brackish assemblage: it includes (i) the euryhaline and eurythermic *Cyprideis torosa*, living in quiet water and tolerating stressed environment (Pascual and Carbonel 1992); (ii) *Loxoconcha elliptica*, preferring phytal environments and hydrodynamic conditions (Oh and Carbonel 1978; Carbonel and Pujos 1981); and (iii) *Cythermorpha fuscata*, known to dwell in oligo- to mesohaline waters. The abundance of *C. torosa* indicates the closure of environment, while *L. elliptica* marks estuarine and phytal environments (Carbonel 1980).

Lagoonal assemblage: including *Xestoleberis aurantia*, *Leptocythere fabaeformis*, *Leptocythere pellucida*, and the phytal species *Xestoleberis dispar.* These ubiquitous opportunistic forms colonize the coastline system from the mediolittoral zone. They tolerate slight changes in water salinity (Carbonel 1982).

Coastal assemblage: including *Loxoconcha rhomboidea*, *Aurila convexa*, and *Aurila prasina.* It contains the species adapted to agitated environments. They essentially colonize the mediolittoral and the upper limit of the infralittoral zone (Nachite et al. 2013).

Marine assemblage: containing phytal species, such as *Semicytherura incongruens*, *Paracytheridea depressa*, *Callistocythere discrepans*, *Neocytherideis fasciata*, *Hiltermannicythere emaciata*, and *Carinocythereis carinata*, which live in shallow marine waters (Lachenal 1989).

Core and outcrops biofacies

The ostracod and mollusk association proportions, the biocenotic parameters, and the diversity index coupled with sedimentologic data allowed the characterization of eight biofacies and associated environments, named as follows (Table 3):

− *WOLBF* (widely opened lagoon biofacies) is made up of shelly dark silts and shelly coarse sands rich in lithoclasts, mollusks, and ostracods. The marine (35%), coastal (20%), and lagoonal (45%) ostracod assemblages are associated with reduced brackish taxa (10%). Indeed, the species richness (15 taxa), the Shannon (*H*), and the equitability index (*E*) give high values. However, the enhancement of brackish taxa (50%) and the depletion of lagoonal (30%), marine (15%), and coastal (10%) assemblages mark the estuarine influence (core C3). This biofacies is also characterized by the reduction of the species (9 taxa) and individuals number (50 ind.)

− *BELBF* (brackish estuarine lagoon biofacies) includes coarse sands and silty clays where the ostracods are subdivided into dominant brackish (95%), lagoonal (3%), and marine-coastal assemblages (2%). The brackish association is characterized by the dominating species *C. torosa* (100%). The mollusks show the dominance of lagoonal assemblages (90%). The importance of individual number and the increase of faunal estuarine assemblages indicate the richness of the realm in nutrients brought by El Achaach watercourse and the maximum of estuarine influences (C3 and C1S). However, in C4 core, the depletion of brackish assemblages (50%) associated to the enhancement of the marine,

Table 3 Dominant ostracod and mollusk associations and taxa, biocenotic parameters, diversity index, and sedimentologic signatures of biofacies and associated environment

Biofacies	Opened embayment (OEBF)	Tsunami (TEBF)	Brackish estuarine lagoon (BELBF)	Widely opened lagoon (WOLBF)	Shallow littoral (SLBF)	Closed lagoon (CLBF)	Emerged (ELBF) / Sebkha (SBF)
Characteristics	High ← Important ← Opened ←			Fresh water influence / Energy waves / Communication			→ Low → weak → Closed
Dominant ostracods and mollusks associations and taxa	- Brackish ostracod: *C. torosa* (100%) - Marine mollusks (40 %) - Lagoonal mollusks (60%) - Mollusk fragments (75%)	- Brackish ostracods (75%): *C. torosa* (95%), *L. elliptica* (5%) - Lagoonal (10%), marine (10%) and coastal ostracods (5%) - Marine mollusks (25%) - Lagoonal mollusks (75%)	- Brackish ostracods (95%): *C. torosa* (100%) - Lagoonal (3%), marine (1%) and coastal ostracods (1%) - Marine mollusks (10%) - Lagoonal mollusks (90%) Maximum estuarine influences (C3 and C1S cores) - Brackish ostracods (50%): *L. elliptica* (75 %), *C. torosa* (20%), *C. fuscata* (5%) - Lagoonal(30%), marine (10%) and coastal ostracods (10%) - Marine mollusks (35%) Limited estuarine influences (C4 core)	- Brackish ostracods(10%): *C. torosa* (45%) *L. elliptica* (45%), *C. fuscata* (10%) - Lagoonal (45%), marine (35%) and coastal ostracods (20%) - Marine mollusks (30%) - Lagoonal mollusks (70%) Maximum pelagic influences (C4 core) - Brackish ostracods (50%), *C. torosa* (80%), *L. elliptica* (10%) and *C. fuscata* (10%) - Lagoonal (30%), marine (15%) and coastal ostracods (5%) - Marine mollusks (20%) Limited pelagic influences (C3 core)	- Brackish ostracods (75%): *C. torosa* (90%) and *L. elliptica* (10%) - Lagoonal (10%), marine +coastal ostracods (15%) - Marine mollusks (20%) - Lagoonal mollusks (80%) Estuarine influences	- Brackish ostracods: (85%): *C. torosa* (95%), *L. elliptica* (1%), *C. fuscata* (4%) - Lagoonal ostracods (15%): *L. pellucida* (70%) and X. aurantia (30%)	- No ostracods - No mollusks
Population structures, biocenotic parameters and diversity index	- Mollusk fragments (75 %) - Presence of a Senegalese mollusks, filled with sediments, such as *Glycymeris violascescens, Cerithium vulgatum, Cerastoderma, glaucum and Strombus bubonius* in coastal outcrops	- High values of species number and density (C4 core) - Just adults for some species and juvenile for others - Broken ostracods valves and angular fragments - Shell bed rich in articulated bivalvia	- Less values of species number - Low values of diversity index (H and E) - High values of individual number except C4 core - Increase of faunal estuarine assemblages - Rich nutrients	- High values of species number and density - High values of diversity index (H and E) - High percentage of broken mollusk (80%)	- High values of density and species number - High values of H and E index - Recurrence of ostracofauna	- Reduction of abundance and species number - Disappearance of mollusks	- Low energy - Regressive period
Sedimentologic signatures	- White quartz rich sands	- Very coarse sands - Richness in charcoal particles, pottery fragments - Erosional contact - Fining up-ward sequence - Extension inland (160 m)	- Silty clay / Coarse sands - High energy - High quartz grain number - Genesis of sandy spits	- Dark silts - High number of lithoclasts - Fining up-ward sequence - Erosional base - Coarser sand comparing to the underlying unit	- Sands rich in phanerogams (C3 core) - Silts and clays (C4 core)	- Fine sands - Protected by sand spits	- Fine sands / dark silts - Aeolian deposits
Morphology	-Developped embayment	- Destruction of sandy spits - Deep channels and intertidal zone	- Elangated barrier - Deep channels	- Wide passes - Short separated barriers	- Narrow passes - Short barrier	- More narrow passes - Elongated barrier	- Absence of passes - Contained sand spits
Ocean/lagoon exchange	- Important	- Important	- limited	- Important	- middle	- Limited	- absent

lagoonal, and coastal assemblages attests a limited estuarine influence (Pascual and Carbonel 1992).

− *SLBF* (shallow littoral biofacies), recorded in C3 and C4 cores, consists of sands, rich in phanerogams, silts, and clays. It is characterized by marine–coastal (15%), brackish (75%), and lagoonal (10%) ostracods association and reveals high values of *H* and *E* diversity index and of biocenotic parameters.

− *CLBF* (closed lagoon biofacies) is built up by fine sands rich in brackish ostracods (85%) accompanied by lagoonal species (15%). The brackish assemblage contains *L. elliptica* (5%), *C. torosa* (85%), and *Cyteromorpha fuscata* (10%) which characterize low energy of environment and an elevated ion concentration. CLBF gives low values of individual number and species richness.

− *TEBF* (tsunami event biofacies). This peculiar biofacies, made up by fining-upward and thinning-landward sequence, is subdivided in two categories: the first one corresponds to shelly coarse sands rich in articulated bivalvia, angular sharpened fragments and characterized by an erosional contact. The shell beds are characterized by the predominance of the lagoonal taxa *Cerithium vulgatum* (Khadraoui et al. 2018).

The second biofacies is built up by silts rich in terrestrial material. Ostracods are subdivided into brackish (75%), lagoonal (10%), coastal (5%), and marine (10%) assemblages. *C. torosa* (95%) is more abundant than *L. elliptica* (5%). Likewise, the population is characterized by high values of density and species richness and by the abundance of broken valves. The population structure shows the dominance of juvenile valves for some species and adult ones for others, which indicates their allochthonous character and thus their deposition under a tsunami event (Khadraoui et al. 2018).

− *OEBF* (opened embayment biofacies) is made up of typical white quartz sands rich in well-preserved and fragmented mollusks. The OEBF is characterized in cores by the dominance of the brackish *C. torosa* (100%) and the lagoonal mollusks (60%). Trenches and outcrops series show the presence of mollusk shells filled with sediments, such as the Senegalese gastropods *Persististrombus latus* and *Conus mediterraneus* associated to *Glycymeris violacescens*, *Cerithium vulgatum*, *Cerastoderma glaucum*, *Dentalium* sp., and *Natica* sp.

− *ELBF* (emerged lagoon biofacies). It is built up by azoic fine sands and clays reflecting low standings of the water in the closed lagoon.

− *SBF* (sebkha biofacies). This biofacies is characterized by silts void of macro- and microfauna. It represents the surface sediments of the studied area.

El Merdassia cores biofacies

C3 core

Along C3 core, ostracods reach 200 ind. 10 g^{-1} and 8 species. They are mainly represented by the brackish *C. torosa* (87%), followed by the lagoonal *L. fabaeformis* (6%) and the coastal *Cushmanidea elongata* (2%). The lagoonal mollusks *Cerithium vulgatum* and *Hydrobia ventrosa* are dominant,

reaching up to 27 and 24%, respectively. However, the marine taxa *Conus mediterraneus* and *Dosinia lupinus* represent 23 and 9%, respectively. The vertical distribution of ostracod and mollusk taxa coupled with their biocenotic parameters along C3 core allowed us to distinguish six biofacies covering the Upper Pleistocene–Holocene interval (Figs. 4 and 5, Table 3).

OEBF, from 131 to 100 cm: This monospecific biofacies shows the dominance of the brackish euryhaline taxon *C. torosa* in some levels. Marine mollusks (40%) associated to dominant lagoonal taxa (60%), such as *Cerithium vulgatum* and *Hydrobia ventrosa*, and the high percentage (75%) of mollusk fragments characterize the upper part of the interval. This biofacies is also characterized by the dominance of the coastal foraminifera *Quinqueloculina seminula* (40%). Several trenches dug near C3 and coastal outcrops show the presence of a rich mollusk taxa such as *Glycymeris violascescens*, *Cerithium vulgatum*, *Cerastoderma glaucum*, and *Dentalium* sp., associated to the Senegalese *Persististrombus latus* Gastropoda. This assemblage is commonly mentioned in outcrops along the Tunisian coast and considered as an important stratigraphic marker of marine isotope stage (MIS 5.5) (Paskoff and Sanlaville 1983; Jedoui 2000).

WOLBF, from 100 to 83 cm, is distinguished from the previous biofacies by its richness with clean mollusks without sediment filling. The well-preserved shells give the age 2225 years cal BP. The lithological sequence, rich in lithoclasts and mollusk fragments (80%), is developed with a fining-upward positive trend. The sands have an erosional base and are coarser compared to the underlying biofacies. They reveal the increase of ostracod and mollusk species in number and density and of coastal foraminifera reaching 70% for the taxa *Quinqueloculina laevigata*. In addition, the widely opened lagoon biofacies records the presence of coastal (12%), marine (15%), and lagoonal (28%) ostracod assemblages associated to the brackish one (45%). Besides, equitability and Shannon indices of ostracods and mollusks give high values.

BELBF, from 83 to 63 cm, made up of sands (U3), is marked by the impoverishment of coastal foraminifera and of lagoonal, marine, and coastal ostracod relieved by the enrichment of the brackish assemblage which becomes dominant (100%). The dominance of lagoonal mollusks, the low values of ostracod and mollusk species number and diversity index (*H* and *E*), and the high density of ostracods characterize the BELBF. The latter also reveals the abundance of quartz grains, coupled with the dominance of the brackish *C. torosa*, which suggests their continental origin. All these parameters exhibit the installation of a brackish estuarine lagoon evolving to the closure (CL).

ELBF, from 63 to 38 cm, is made up of silts (U4) and clays (U5) without macro- and microfauna.

SLBF, from 38 to 20 cm, is made up of sands characterized by their richness with phanerogams and by the abrupt recurrence of ostracods and lagoonal and coastal foraminifera. The dominant brackish *Cyprideis torosa* is associated to the lagoonal *Leptocythere fabaeformis* and *Leptocythere* sp. and to the coastal *Loxoconcha rhomboidea*, *Aurila convexa*, and

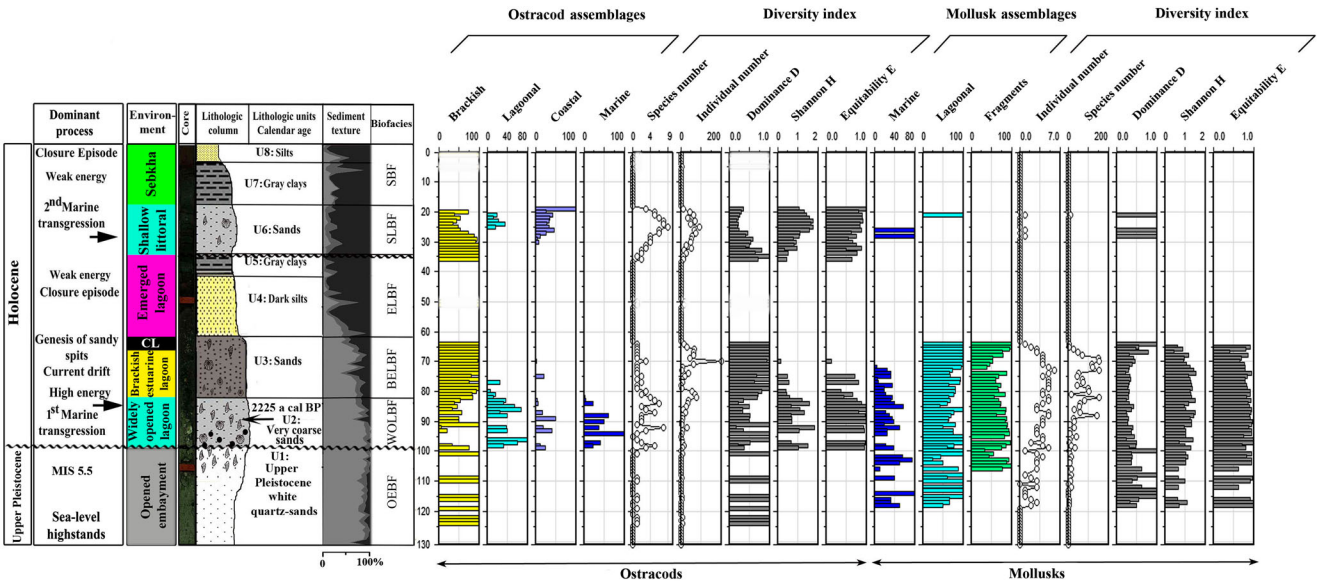

Fig. 4 Sedimentologic, ostracod, and mollusk data of C3 core. Dominant process, environments, lithologic column, lithologic units/calendar median age in years BP, sediment texture (< 63 μm represented in black, > 63 μm represented in dark gray and > 125 μm represented in light gray), biofacies, vertical distribution of ostracod and mollusk associations, and biocenotic parameters (diversity index: *H*, *E*, and *D*)

Fig. 5 Lithologic column, lithologic units, calendar median age in years BP, sediment texture (< 63 μm represented in black, > 63 μm represented in dark gray and > 125 μm represented in light gray), biofacies, and vertical distribution of foraminifera taxa of C3, C1s, and C4 cores

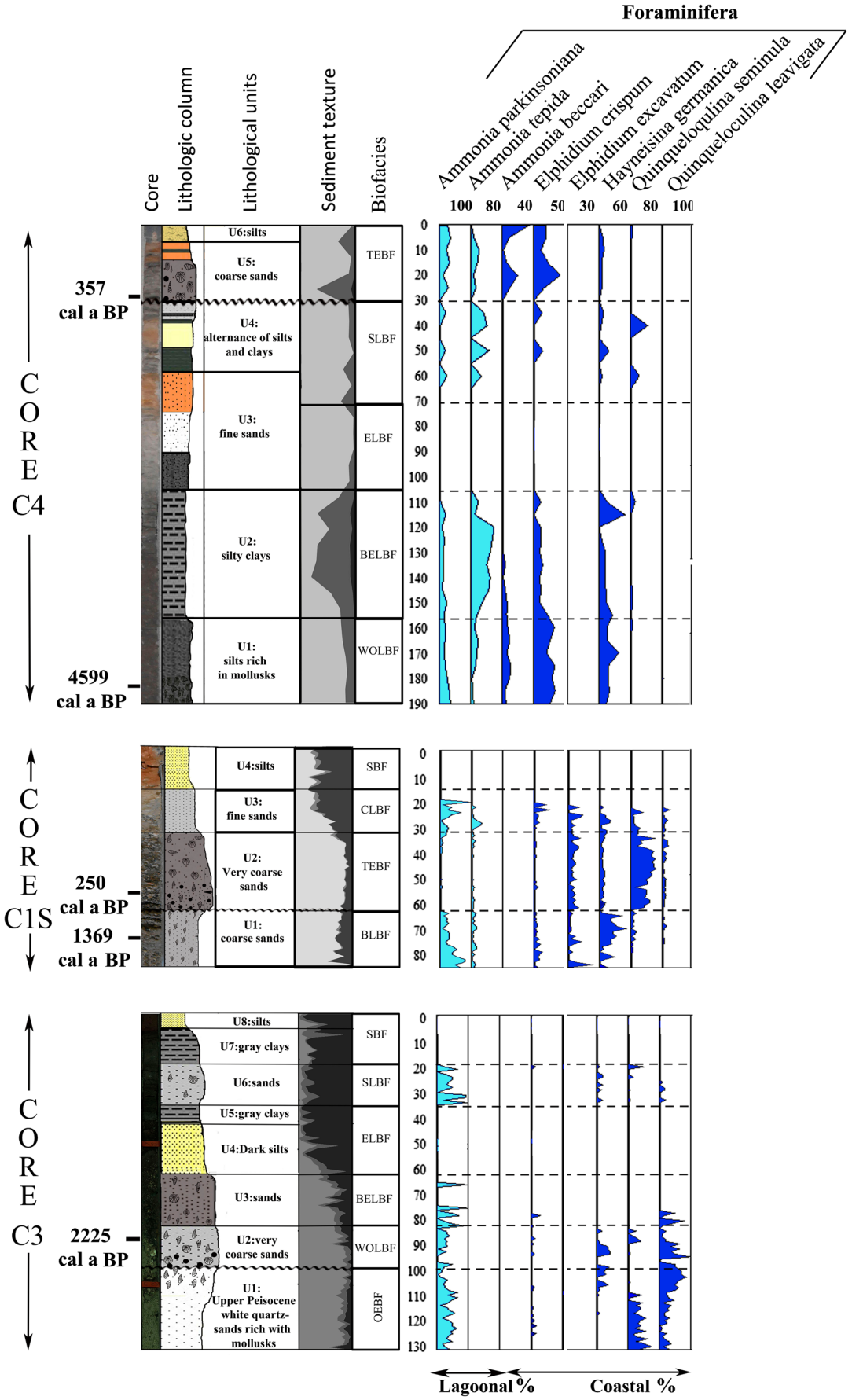
Foraminifera
Ammonia parkinsoniana
Ammonia tepida
Ammonia beccari
Elphidium crispum
Elphidium excavatum
Hayneisina germanica
Quinqueloqulina seminula
Quinqueloculina leavigata
100 80 40 50 30 60 80 100
Core
Lithologic column
Lithological units
Sediment texture
Biofacies
CORE C4
357 cal a BP
4599 cal a BP
U6:silts
U5: coarse sands
U4: alternance of silts and clays
U3: fine sands
U2: silty clays
U1: silts rich in mollusks
TEBF
SLBF
ELBF
BELBF
WOLBF
CORE C1S
250 cal a BP
1369 cal a BP
U4:silts
U3: fine sands
U2: Very coarse sands
U1: coarse sands
SBF
CLBF
TEBF
BLBF
CORE C3
2225 cal a BP
U8:silts
U7:gray clays
U6:sands
U5:gray clays
U4:Dark silts
U3:sands
U2:very coarse sands
U1: Upper Peisocene white quartz-sands rich with mollusks
SBF
SLBF
ELBF
BELBF
WOLBF
OEBF
Lagoonal %
Coastal %

Callistocythere discrepans. To the top of the interval, the brackish taxa become poor and the lagoonal and coastal taxa grow. Besides, biocenotic parameters and diversity index *H* and *E* give high values. All these parameters explain the installation of a shallow littoral environment.

SBF, from 20 cm to the surface, built up with gray clays and silts, is characterized by the absence of ostracods and mollusks.

C1S core

Ostracods are more abundant (700 ind. 10 g^{-1}) than in C3 core, but they give a comparable number of taxa. The brackish *C. torosa* is dominant (80%), followed by the two lagoonal *L. pellucida* (5%) and *L. fabaeformis* (4%). The marine and coastal species do not exceed 3%.

It reveals four biofacies, which register a transgression and a tsunami event (Figs. 5 and 6, Table 3).

BLBF, from 85 to 64 cm, constituted of coarse sands, encloses brackish gastropods, such as *Hydrobia ventrosa*, which gives the ^{14}C age 1396 years cal BP. It is characterized by the dominance of the brackish *Cyprideis torosa* and the lagoonal foraminifera *Ammonia parkinsoniana* (80%). To the top, the lagoonal, marine, and coastal ostracod species increase slightly at the expense of the brackish taxa. The enrichment of the three associations is related to the increase of species number and the reduction of the density. Likewise, the values of *H* and *E* indices increase in the upper part of the interval.

TEBF, from 64 to 36 cm, is made up of very coarse sands (U2) rich in lithoclasts and mollusks 250 years cal BP in age. This unit shows a fining-upward sequence with an abrupt basal erosional contact. It also displays that ostracod assemblages are mostly diversified within the entire core. Eight species, belonging to four assemblages, are herein present. The abrupt enrichment of the coastal and marine ostracod assemblages and of the coastal foraminifera *Q. seminula* (60%) characterizes the lower limit of the interval. Likewise, the ostracod species numbers supply the highest values along the core. The high values of (*H*) and (*E*) ostracod indices show a more important marine influence than in the previous biofacies. The population structure reveals that marine ostracod taxa are only in juvenile forms for some species and only adults for others. Laprida (2001) notes that only populations with juvenile/adult ratios varying between 3/1 and 5/1 have a probability of being in situ. However, the marine species would therefore be displaced with regard to the hydrodynamics of the environment and indicate a strong marine current influence. In addition, broken valves of ostracods prove the tsunami event.

CLBF, from 36 to 24 cm, built up of fine sands, is marked by the decrease of ostracod species and individual number and by the absence of mollusks. The lagoonal and coastal ostracod depletion and then their disappearance are relieved by the enrichment of the brackish taxa *C. torosa* (100%).

The increase of the lagoonal foraminifera *A. parkinsoniana* (60%) and the brackish *C. torosa* taxa, the high values of dominance coupled with the decrease of species number and density observed at the top of the interval note the settlement of a lagoon and its progressive closure.

SBF, from 24 cm to the top, is characterized by the development of azoic silt levels.

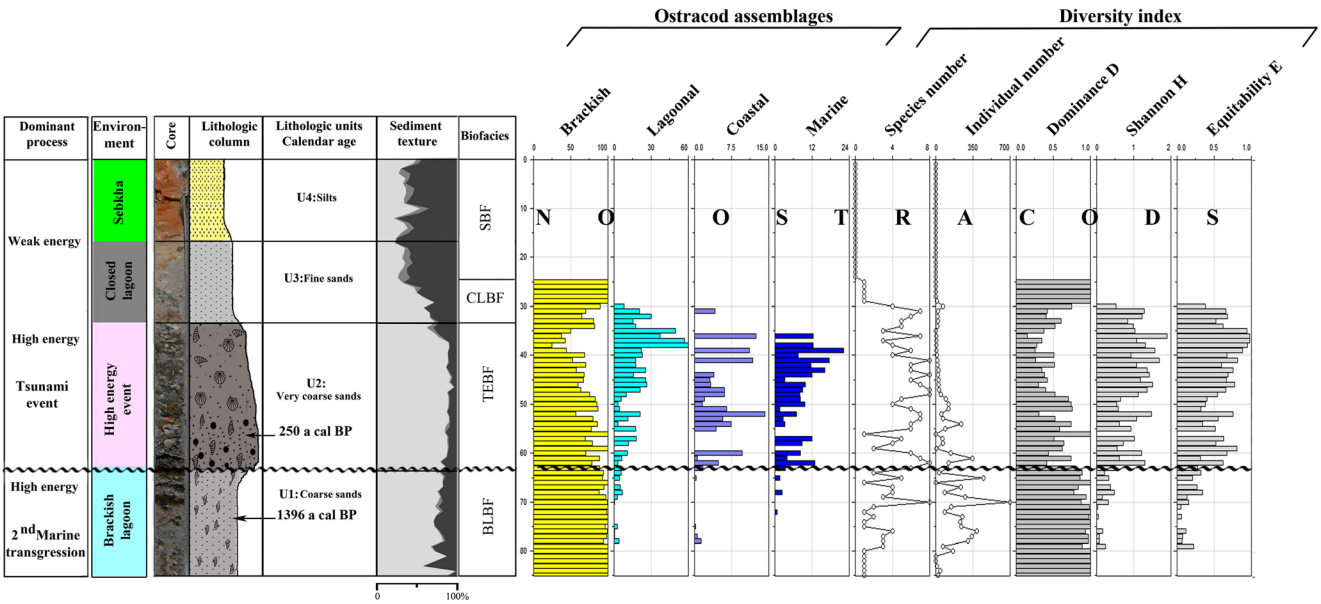

Fig. 6 Sedimentologic, ostracod data of C1s core. Dominant process, environments, lithologic column, lithologic units/calendar median age in years BP, sediment texture (< 63 μm represented in black, > 63 μm represented in dark gray and > 125 μm represented in light gray), biofacies, vertical distribution of ostracod taxa, species number, and density

C4 core

Ostracods are more diversified than in C3 and C1S cores, and they reach up to 18 species. The brackish ostracod *C. torosa* reaches the highest percentage along C4 core (41%) followed by the two lagoonal *Xestoleberis aurantia* (11%) and *Leptocythere fabaeformis* (8%). Ostracod and mollusk assemblages, species richness, individual number, and diversity index allowed the recognition of five successive biofacies in this core (Figs. 5, 6, and 7, Table 3).

WOLBF, from 190 to 155 cm, is made up by dark silts rich in mollusks 4599 years cal BP in age. This biofacies shows the dominance of coastal foraminifera assemblage represented by *Elphidium crispum* (40%) and *Hayneisina germanica* (30%). It includes 18 ostracod species and reveals the dominance of lagoonal assemblage (50%), associated to marine (20%), brackish (15%), and coastal (15%) ones. The marine assemblage is mainly represented by *Semicytherura incongruens*, *Hiltermannicythere emaciata*, and *Carinocythereis carinata*. Also, this biofacies gives the highest values of ostracod species richness, density, and diversity indices *H* and *E*. In addition, the mollusks show the dominance of the lagoonal assemblage (80%) and high values of species richness and density.

BELBF, 155 to 105 cm, made up of silty clays, is marked by the decreases of the values of the biocenotic parameters of mollusks and ostracods. The latter contain dominant brackish assemblage followed by the lagoonal, coastal, and marine ones. In the brackish assemblage, the dominant *L. elliptica*, which prefers higher hydrodynamic conditions and estuarine environments, is associated to *C. torosa*. The lagoonal foraminifera *Ammonia tepida* increase herein and reach 70%. The mollusks are marked by the enrichment of marine taxa. The upper part of the interval is characterized by the enhancement of the brackish ostracod assemblage coupled with the impoverishment of the coastal, lagoonal, and marine taxa. In the brackish assemblage, *L. elliptica* reveals a reduction in its percentage, indicating the decrease of environment energy. The reduction of the energy is also proved by the high percentage (80%) of the fine fraction (< 125 μm). All these parameters indicate a brackish estuarine lagoonal environment evolving to the closure. In fact, from 115 to 105 cm, the enhancement of *C. torosa* which reaches 100% is associated to the reduction of the density, the species richness, and the two diversity indices (*H* and *E*), and the increase of the number of quartz grains mark the closure of the lagoon (CL).

ELBF, from 105 to 70 cm, is characterized by the absence of microfauna and macrofauna in the fine sands of U3.

SLBF, from 70 to 35 cm, is constituted by the upper part of the sands of U3 and by silts and clays of U4. It exhibits the reappearance of ostracods. The lagoonal foraminifera *A. tepida* (30%) and *A. parkinsoniana* (15%) and the coastal *Quinqueloculina seminula*, *Elphidium crispum* (25%), and *Haynesina germanica* (30%) recur. To the top, marine and coastal ostracod species appear, the species richness and density of ostracod increase, and the lagoonal mollusks recur, such as *Hydrobia ventrosa* and *Abra alba*. All these parameters indicate the settlement of a shallow littoral environment.

TEBF, from 35 cm to the surface, is made up of very coarse sands (U5) and silts (U6). The coarse sands, arranged in a fining-upward sequence, contain rich mollusk taxa giving the age 357 years cal BP. Upper Pleistocene lithoclasts, charcoal particles, and pottery fragments highlight the erosional contact, which characterizes the basal limit of the interval. This limit is also distinguished by the abrupt increase of marine (18%), lagoonal (12%), and coastal (8%) ostracod assemblages and of the coastal foraminifera taxa *Elphidium crispum* and *Ammonia beccari.* TEBF shows high values of species numbers, diversity index and density of ostracods and mollusks, and the development of

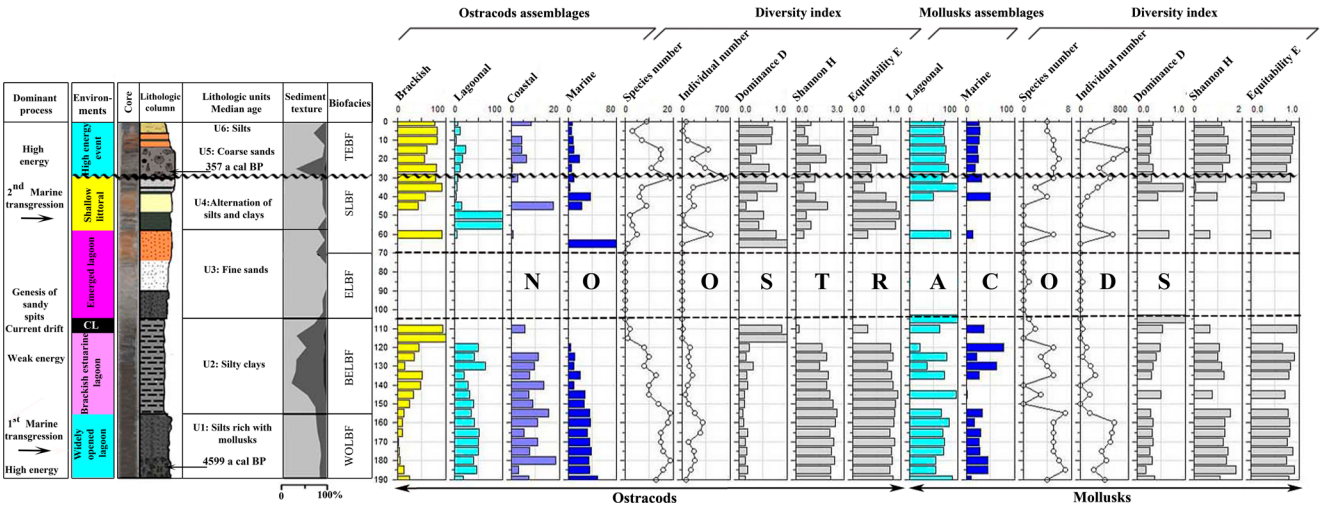

Fig. 7 Sedimentologic, ostracod data of C4 core. Dominant process, environments, lithologic column, lithologic units/calendar median age in years BP, sediment texture (< 63 μm represented in black, > 63 μm represented in dark gray and > 125 μm represented in light gray), biofacies, vertical distribution of ostracod and mollusk associations, and biocenotic parameters (diversity index: *H*, *E*, and *D*)

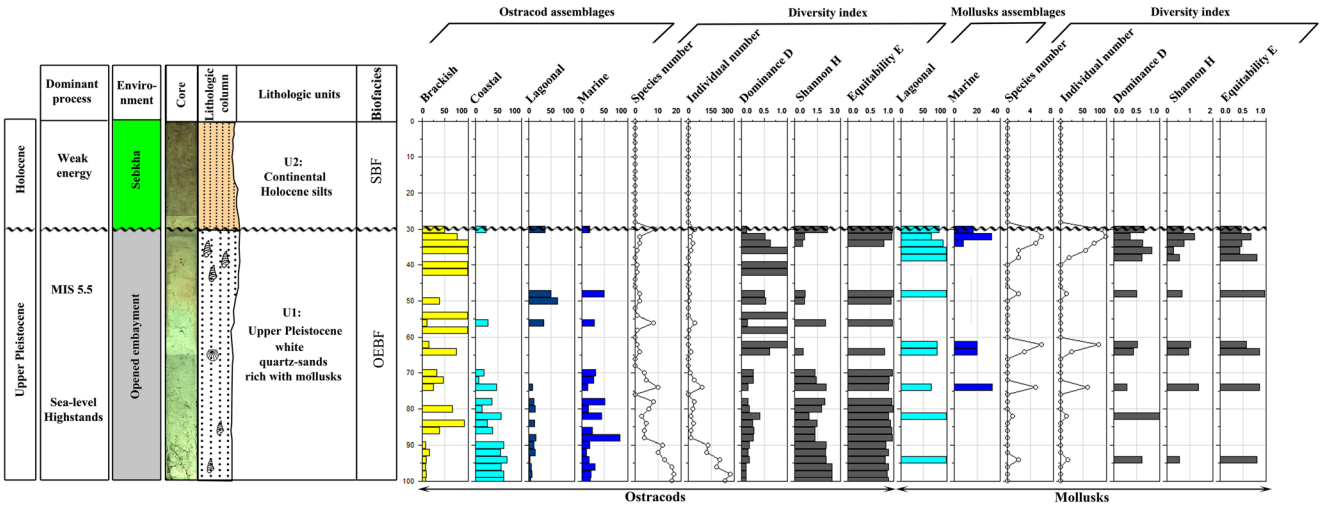

Fig. 8 Ostracod and mollusk data of C5 core. Dominant process, environments, lithologic column, lithologic units, biofacies, vertical distribution of ostracod and mollusk associations, and biocenotic parameters (diversity index: *H*, *E*, and *D*)

broken marine mollusks (50%). The simultaneous presence of the phytal *L. elliptica* signifies a high-energy environment (Viehberg et al. 2008), and the brackish euryhaline and eurythermal dominant *C. torosa*, which characterizes a low energy, signifies a high energy and the reworking of the taxa *C. torosa*.

El Awebed core and outcrops biofacies

C5 and C6 cores

OEBF, from 100 to 30 cm (C5) and from 100 to 43 cm (C6), is made up of white quartz sands, Upper Pleistocene in age, rich in mollusks and pebbles (Figs. 8 and 9). This biofacies shows the dominance of the brackish euryhaline taxa *C. torosa*. Lagoonal, coastal, and marine associations are also present in some levels. Dominant lagoonal mollusks (80%) are associated to marine taxa (20%), such as *Cerithium vulgatum* and *Hydrobia ventrosa*. Several trenches dug near C5 and C6 and coastal outcrops show the presence of the Senegalese mollusks whose shells are filled with sediments, such as *Persististrombus latus* and *Conus mediterraneus*. This assemblage is commonly mentioned in the Upper Pleistocene outcrops present along the Tunisian coast (Paskoff and Sanlaville 1983; Jedoui 2000).

SB, from 30 cm to the top (C5) and from 43 cm to the top (C6), is characterized by the development of azoic continental Holocene silts and silty sands.

Outcrops

Henchir El Mejdoul cross section

The TEBF can be subdivided by means of paleontological and sedimentological criteria in two categories: uprush biofacies (UBF) and backwash biofacies (BBF) (Fig. 10).

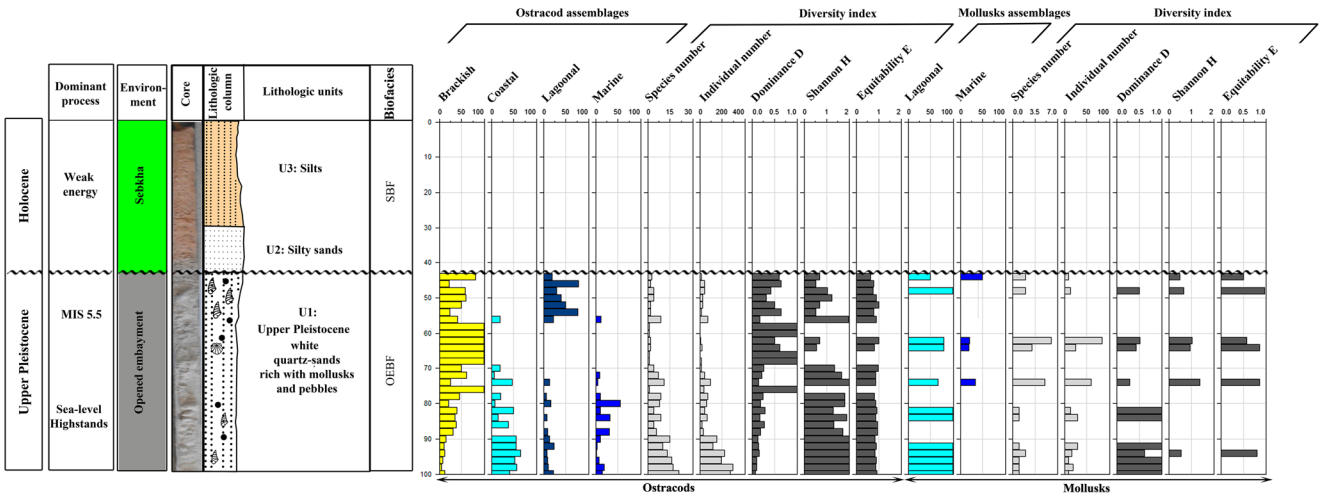

Fig. 9 Ostracod and mollusk data of C6 core. Dominant process, environments, lithologic column, lithologic units, biofacies, vertical distribution of ostracod and mollusk associations, and biocenotic parameters (diversity index: *H*, *E*, and *D*)

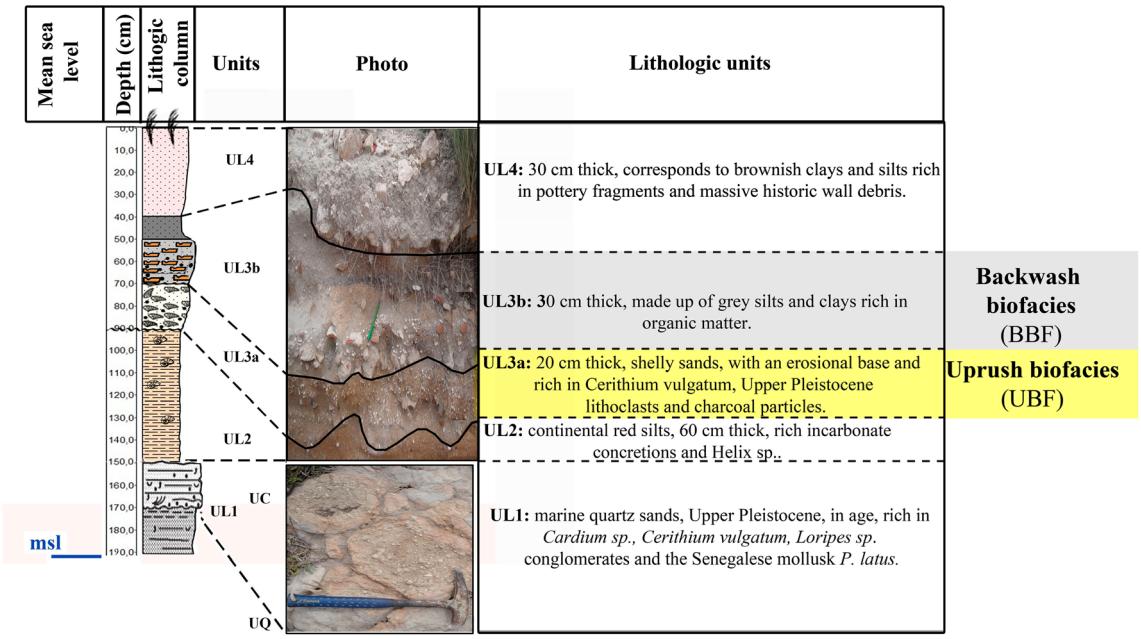

Fig. 10 Log of Henchir El Mejdoul outcrops showing the different lithological units (UL1, UL2, UL3a, UL3b, and UL4) and the two biofacies Uprush and Backwash

The UBF is made up of shelly sands rich in *Cerithium vulgatum*, showing an erosional base and organized in a fining-upward sequence. It also contains lithoclasts, Upper Pleistocene in age, and charcoal particles. This biofacies rises up to 0.75 m in altitude and outcrops up to 160 m in land, thins progressively, and disappears. The taphonomic results of the *Cerithium* shells reveal a dissolved surface and deteriorated tubercles and their filling with silts, which attest their allochthonous origin. However, the remaining dominant *Cerithium vulgatum* shells are rather sharpened and void of sediment, which proves their Holocene origin. This biofacies is also characterized by the dominance of articulated Bivalves (*Glycymeris* sp., *Loripes* sp., *Cardium* sp.) and high proportion of reworked sharpened Holocene bioclasts. The mixture of Holocene and dominant Upper Pleistocene foraminifera characterized by dissolved and corroded test surface reveals the high energy of the environment.

This peculiar biofacies (BBF) is characterized by its richness in organic matter and is organized in fining-upward and thinning-landward sequence. In the west of Henchir El Mejdoul, it overlies directly the continental silts rich in *Helix* sp. and carbonate concretion by an erosional contact. The latter is highlighted by decimetric pottery fragments, charcoal particles, muddy rip-up clasts, and boulders.

Discussion

Correspondence analysis

To clarify the results of the descriptive study, a correspondence analysis (CA), based on ostracod data (brackish, lagoonal, coastal, and marine assemblages; taxa; individual number; and species richness), mollusk variables (lagoonal and marine assemblages, individual number, and species richness), and sampling levels, was carried out. We chose the cores C3 and C1S because of their richness in ostracods and mollusks. For the two cores, CA displays, on the first factorial plan having a maximum of inertia of 62%, a Guttman effect (Benzécri 1980) related to the exposure to the marine influence and, therefore, its energy. It reflects an environmental gradient with variables divided into several groups representing a typical parabolic form.

Core C1S

Variable representation on the factorial plan (F1 × F2) shows clouds of points where three groups can be distinguished (Fig. 11). Group G1 is positioned in the negatives axes F1 and F2. It includes the ostracod individual number, the brackish species *Cyprideis torosa*, and the marine taxa *Paracytheridea depressa.* This group corresponds to the sands of unit 1 and corresponds to a brackish lagoon biofacies. Group G2, located in the positive axes F1 and F2, contains the ostracod species richness and the lagoonal, marine, and coastal ostracod assemblages. It includes rich ostracod taxa such as the brackish *Cytheromorpha fuscata*; the lagoonal species *Xestoleberis aurantia*, *Leptocythere fabaeformis*, *Leptocythere pellucida*, and *Leptocythere* sp.; the coastal taxa *Cushmanidea elongata*, *Loxoconcha rhomboidea*, and *Aurila prasina*; and the marine *Semicytherura incongruens* and *Hiltermannicythere emaciata.* It corresponds to the coarse

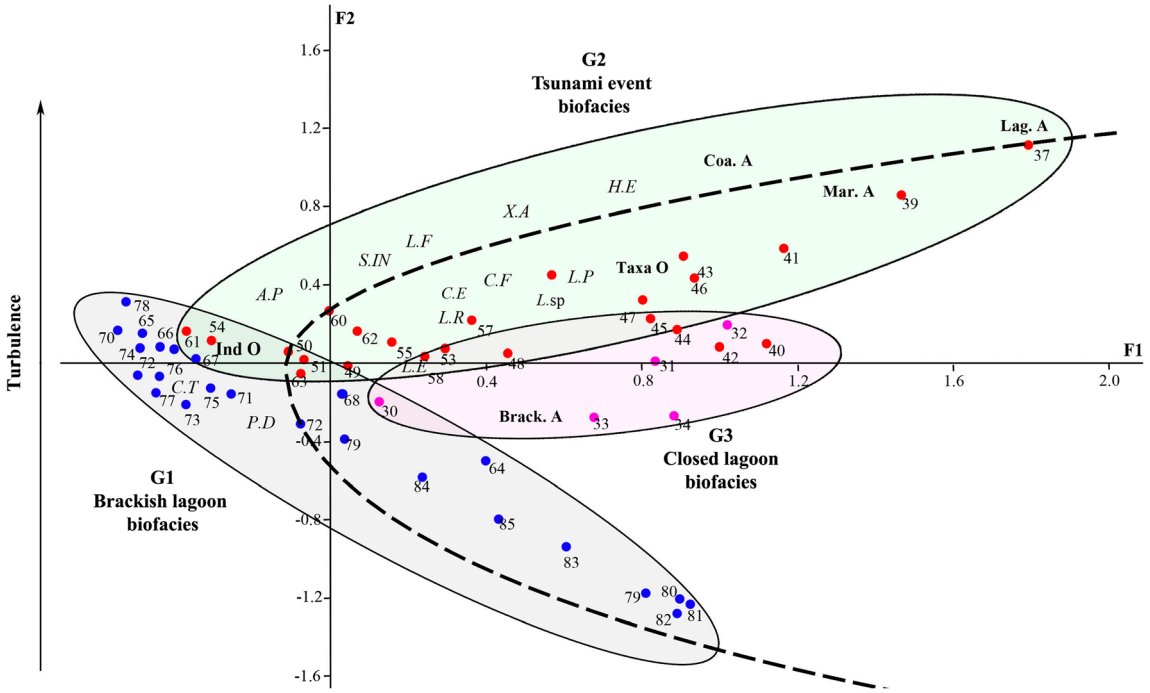

Fig. 11 Factorial correspondence analysis. Projection of ostracod data (absolute abundance, assemblages, species, and individual number) and mollusk data (associations, species and individual number) and samples in the 1 × 2 factorial plane for C1S core

sands of unit U2, marking a tsunami biofacies. The third group G3 contains the brackish assemblage and taxa *Loxoconcha elliptica.* It implies a closed lagoon (U3). Consequently, the axis F2 shows an evolution from a brackish lagoonal (group G1), at its negative pole, toward a peculiar environment (group G2) corresponding to an extreme high-energy tsunami event, at its positive pole, passing by an intermediate closed lagoon (group G3). The axis F2 behaves as the energy factor.

Core C4

Three groups are distinguished (Fig. 12).

The first group G1, located in the positive axis F2 and negative axis F1, contains the brackish *Loxoconcha elliptica*, the lagoonal species *Leptocythere pellucida* and *Leptocythere fabaeformis*, the coastal taxa *Loxoconcha rhomboidea,* and the marine *Basslerites berchoni* and *Semicytherura sella.* This group corresponds to the evolution of a widely opened lagoon to a brackish lagoon exposed to estuarine influences characterized by the dominance of the brackish estuarine high-energy taxa *L. elliptica* represented by the silty clays of the unit U2.

The second group G2, situated at the positive axis F1 and negative axis F2, can be subdivided into two subgroups. The first one G2a contains only the two marine *Semicytherura incongruens* and *Callistocythere discrepans.* The second group G2b contains the ostracod individual number, the brackish *Cyprideis torosa*, the lagoonal *Xestoleberis dispar*, and the marine *Neocytherideis subulata.* The group G2a, corresponding to the upper parts of U3 an U4, indicates a shallow littoral environment. G2b occupying a position that deviates from the previous cloud indicates a peculiar environment corresponding to the extreme high-energy tsunami event proved by descriptive analysis.

The third group G3, situated at the negative axes F1 and F2, contains the mollusk and ostracod species richness and the mollusk individuals number, the lagoonal taxa *Xestoleberis aurantia,* the coastal species *Cushmanidea elongata* and *Aurila prasina* and the marine taxa *Paracytheridea depressa*, *Carinocythereis carinata*, *Hiltermannicythere emaciata*, and *Neocytherideis fasciata.* Group G3 is representative of a widely opened lagoon, corresponding to the unit U1. Both groups G1 and G2, constituting branches of the parabola, are separated in the center by the intermediate group G3. Therefore, the axis F2, which acts as the energy factor of the environment, shows an evolution from a brackish environment (G1) on its positive pole toward an opened lagoon submitted to an extreme high-energy tsunami event, at its negative pole (G2). A widely opened lagoon environment (G3) makes up the transition between the two environments.

Paleoenvironmental reconstruction

The results of paleontological, sedimentological, and geochronological analyses enable us to reconstruct the changing paleoenvironment within the investigated Sfax northern coast and compare this evolution with southern Skhira coast (Zaïbi et al. 2016). Although both areas, belonging to the Gulf of

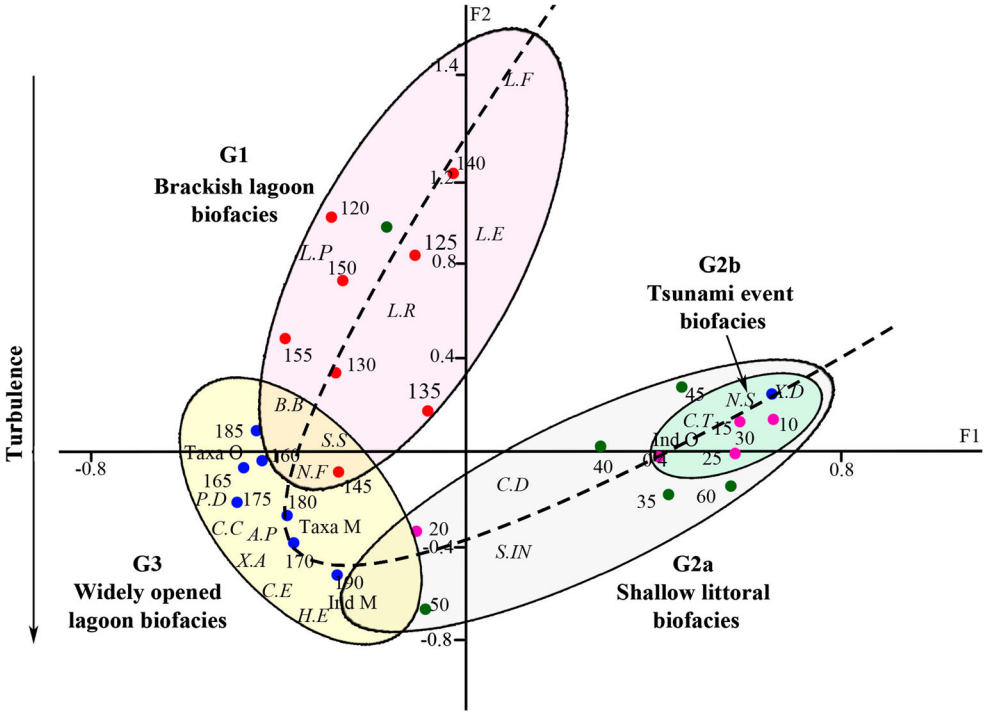

Fig. 12 Factorial correspondence analysis. Projection of ostracod data (absolute abundance, assemblages, species, and individual number) and mollusk data (associations, species, and individual number) and samples in the 1 × 2 factorial plane for C4 core. *Cyprideis torosa* (*C.T*), *Cytheromorpha fuscata* (*C.F*), *Loxoconcha elliptica* (*L.E*), *Xestoleberis aurantia* (*X.A*), *Xestoleberis dispar* (*X.D*), *Leptocythere faba!eformis* (*L.F*), *Leptocythere pellucida* (*L.P*), *Leptocythere* sp. (*L.sp*), *Loxoconcha rhomboidea* (*L.R*), *Aurila convexa* (*A.C*), *Aurila prasina* (*A.P*), *Cushmanidea elongate* (*C.E*), *Basslerites berchoni* (*B.B*), *Hiltermannicythere emaciata* (*H.E*), *Paracytheridea depressa* (*P.D*), *Carinocythereis carinata* (*C.C*), *Semicytherura incongruens* (*S.IN*), *Semicytherura sella* (*S.S*), *Neocytherideis subulata* (*N.S*), *Neocytherideis fasciata* (*N.F*), *Callistocythere discrepans* (*C.D*). Ostracod individual number (Ind O), ostracod species number (Taxa O), mollusk individual number (Ind M), mollusk species number (Taxa M), brackish association (Brack. A), lagoonal association (Lag. A), marine association (Mar. A), coastal association (Coa. A). *C1S core*: blue points: samples from 85 to 64 cm; red points: samples from 63 to 36 cm; pink points: from 35 to 32 cm. *C4 core*: blue points: samples from 190 to 160 cm; red points: samples from 155 to 100 cm; green points: samples from 75 to 35 cm; pink points: samples from 30 cm to the surface

Gabes, are subject to the same forces, the response may vary or be different over time. In the following section, the development of the investigated areas is discussed in three phases: (i) a pretransgressional substratum, (ii) a sea-level rise as a phase of marine influence and a phase of stagnation of sea level, and (iii) a phase of high energy (Figs. 13 and 14).

Upper Pleistocene to early Holocene pretransgressional substratum

The sea level rose leading to a transgressive deposit at 120 ka. Subsequently, a brief drop of sea level around 40 ka allowed the deposition of colluvian and eolian sediments. It indicates a slowly falling sea level. During the last interglacial, the deposits at the central and south Tunisian coast experienced a drastic change from a quartz- to a carbonate-dominated sedimentation sometime. Littoral sedimentation ceased at 70 ka when the coast became sediment starved in the course of the falling sea level (Mauz et al. 2009). In northern Sfax coast, this transgression allowed the deposition of a marine quartz sands rich in mollusks and containing Senegalese mollusks. This unit rising at 3 m along Jerba coast (Jedoui 2000) was recognized at 14 m depth at Sfax harbor (Despois 1955). It constitutes the bedrock of sebkhas El Merdessia and El Awebed and outcrops along northern Sfax coast. By means of a palynological study, Morzadek-Kerfourn (2002) mentioned the establishment, in the west of the Gulf of Gabes, of sebkhas at the isobaths − 25 and − 28 m, between 28,340 and 21,120 years BP in connection with the aridity and of marine environment at the isobaths − 75 m, around 12,580 years BP. For Goy et al. (1996), the deceleration of relative sea-level rise took place in the Mediterranean littorals at 10,000 years cal BP. However, Morzadek-Kerfourn (2002) noted that a transgression invaded the gulf of Gabes from 9930 years BP. Around 7 ka cal BP, the surface of the ocean was approaching the present level (Lambeck et al. 2002). The sea level is at − 26 m by 5480 BP and reached a maximum around 4630 BP before stabilizing (Morzadek-Kerfourn 2002). In Sfax eastern coastline, the continental shelf is too wide and is characterized by a very weak slope, reaching depths of 10 m at 2 km from the coastline. The oldest subsurface sediments of Sfax northern coast correspond to the Upper Pleistocene marine quartz sands rich

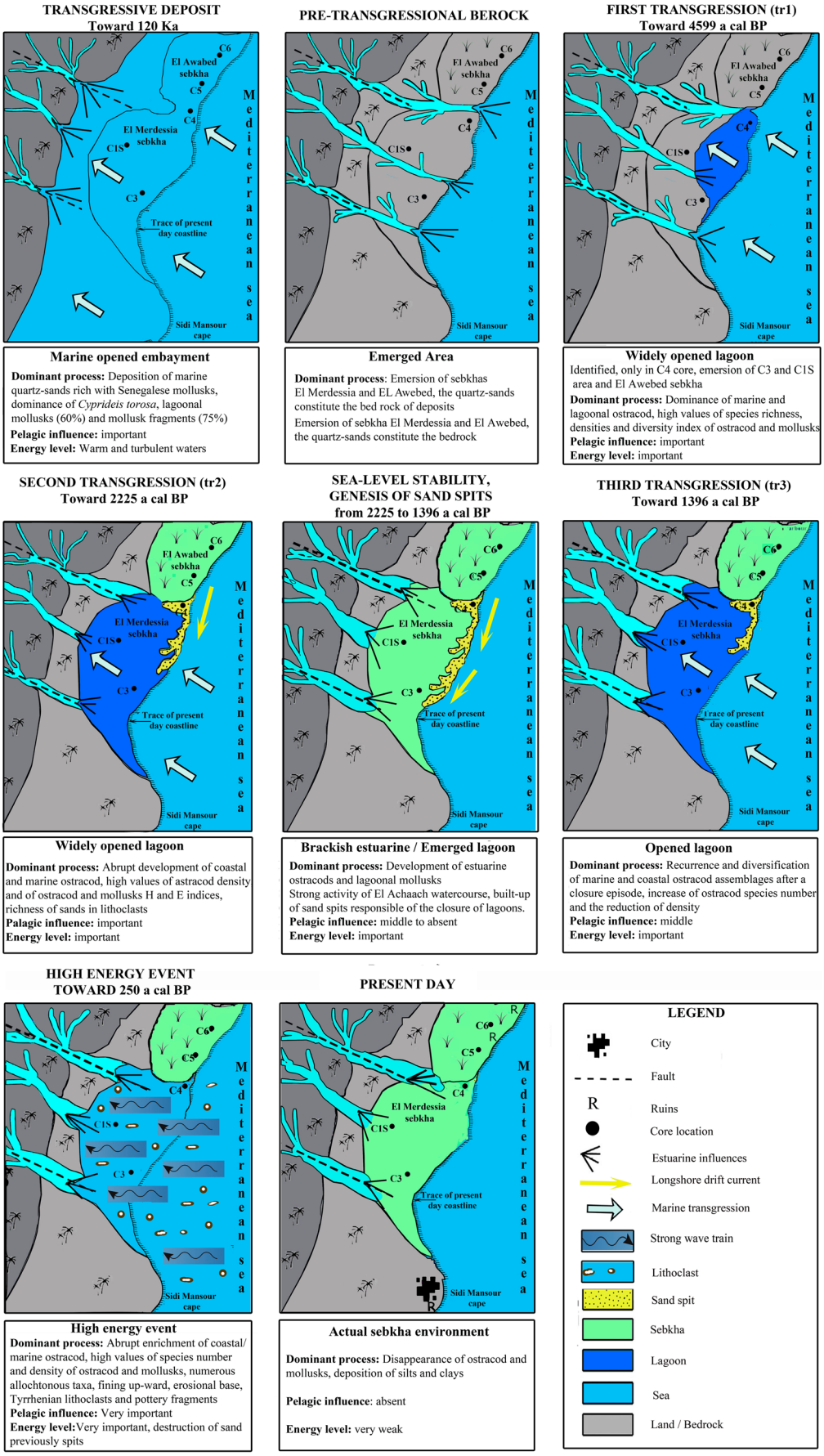
TRANSGRESSIVE DEPOSIT
Toward 120 Ka
PRE-TRANSGRESSIONAL BEROCK
FIRST TRANSGRESSION (tr1)
Toward 4599 a cal BP
El Awabed sebkha
El Merdessia sebkha
C6
C5
C4
C1S
C3
Trace of present day coastline
Sidi Mansour cape
Mediterranean sea
Marine opened embayment
Dominant process: Deposition of marine quartz-sands rich with Senegalese mollusks, dominance of Cyprideis torosa, lagoonal mollusks (60%) and mollusk fragments (75%)
Pelagic influence: important
Energy level: Warm and turbulent waters
Emerged Area
Dominant process: Emersion of sebkhas El Merdessia and EL Awebed, the quartz-sands constitute the bed rock of deposits
Emersion of sebkha El Merdessia and El Awebed, the quartz-sands constitute the bedrock
Widely opened lagoon
Identified, only in C4 core, emersion of C3 and C1S area and El Awebed sebkha
Dominant process: Dominance of marine and lagoonal ostracod, high values of species richness, densities and diversity index of ostracod and mollusks
Pelagic influence: important
Energy level: important
SECOND TRANSGRESSION (tr2)
Toward 2225 a cal BP
SEA-LEVEL STABILITY, GENESIS OF SAND SPITS from 2225 to 1396 a cal BP
THIRD TRANSGRESSION (tr3)
Toward 1396 a cal BP
Widely opened lagoon
Dominant process: Abrupt development of coastal and marine ostracod, high values of astracod density and of ostracod and mollusks H and E indices, richness of sands in lithoclasts
Palagic influence: important
Energy level: important
Brackish estuarine / Emerged lagoon
Dominant process: Development of estuarine ostracods and lagoonal mollusks
Strong activity of El Achaach watercourse, built-up of sand spits responsible of the closure of lagoons.
Pelagic influence: middle to absent
Energy level: important
Opened lagoon
Dominant process: Recurrence and diversification of marine and coastal ostracod assemblages after a closure episode, increase of ostracod species number and the reduction of density
Pelagic influence: middle
Energy level: important
HIGH ENERGY EVENT
TOWARD 250 a cal BP
PRESENT DAY
LEGEND
City
Fault
Ruins
Core location
Estuarine influences
Longshore drift current
Marine transgression
Strong wave train
Lithoclast
Sand spit
Sebkha
Lagoon
Sea
Land / Bedrock
High energy event
Dominant process: Abrupt enrichment of coastal/ marine ostracod, high values of species number and density of ostracod and mollusks, numerous allochtonous taxa, fining up-ward, erosional base, Tyrrhenian lithoclasts and pottery fragments
Pelagic influence: Very important
Energy level:Very important, destruction of sand previously spits
Actual sebkha environment
Dominant process: Disappearance of ostracod and mollusks, deposition of silts and clays
Pelagic influence: absent
Energy level: very weak

◀ **Fig. 13** Hypothesized Holocene paleogeography of northern Sfax coast based on the results of this study focusing on the five cores used for ostracod and mollusk analysis. Dominant process, energy level, and pelagic influence during the main phases of Sfax coast evolution

in mollusks (C3 core) with the absence of continental Holocene series, while the oldest subsurface sediment of southern Skhira coast (Zaïbi et al. 2016) corresponds to a continental early Holocene fine sands and blue clays.

Sea level rises as a phase of marine influences and a phase of stagnation of sea level

First Holocene marine transgression (tr1), 4599 years cal BP in age

This transgression is identified only in C4 core (unit U1); however, the areas of C1S and C3 and sebkha El Awebed remain emerged (Figs. 13 and 14). The presence of the four ostracod associations in U1 sands with the dominance of marine and lagoonal taxa and the high values of species richness and densities of ostracods and mollusks document it. In addition, the pelagic influence is attested by the high values of diversity indices *H* and *E*, which indicate a structured population. All these parameters signify the settlement of a widely opened lagoon. This transgressive event is quoted in the Gulf of Gabes, where the sea level reaches a maximum around 4630 ± 160 years BP before stabilizing (Morzadek-Kerfourn 2002). The Skhira coast (Zaïbi et al. 2016) records the Northgrippien continental sands and clays and two marine transgressions (TR1, TR2), 7460 and 6671 years cal BP in age, which proves the continuity of sedimentation in this area. However, the absence of continental sediments and of the record of the two transgressive events in Sfax coastline can be explained by the uplift behavior of this coast bedrock favored by the activity of the faults visible in northern Sfax area (Fig. 1) unlike the subsidence of the southern Skhira coast.

The second Holocene marine transgression (tr2), 2225 years cal BP in age

This event is marked, in C3 core, by an abrupt increase of lagoonal, coastal, and marine ostracod taxa in the sands overlying the Upper Pleistocene quartz sands. It shows the highest percentage of broken mollusks and high values of ostracod density. The enhancement of ostracofauna and the high values of *H* and *E* indices imply a widely open environment subjected to pelagic influences. In addition, the richness of sands in lithoclasts and their erosional base signify a high-energy deposit. All these parameters register a marine transgression toward 2225 years cal BP. However, the area of sebkha El Awebed remains emerged (Figs. 13 and 14). Tr2 can be correlated with the upper period of the transgressive time event, TR3, 2856 years cal BP in age, described by Zaïbi et al. (2012), in the coast of Skhira where the sedimentation seems to be continued and with that 2700 years BP in age, identified by Paskoff and Sanlaville (1983) in the coast of Zarzis. A similar marine transgression was also recognized along the Spanish coast by Zazo et al. (2008), toward 2400 years cal BP and in the southern Eastern Rhône delta by Vella and Provansal (2000) between 2260 and 1200 years BP. This second event corresponds to a wet period identified by Brun and Rouvillois-Brigol (1985), by means of marine pollen, obtained from the Gulf of Gabes cores where the increase of oak pollen toward 2500 years BP argues in favor of a short period of humidity. Likewise,

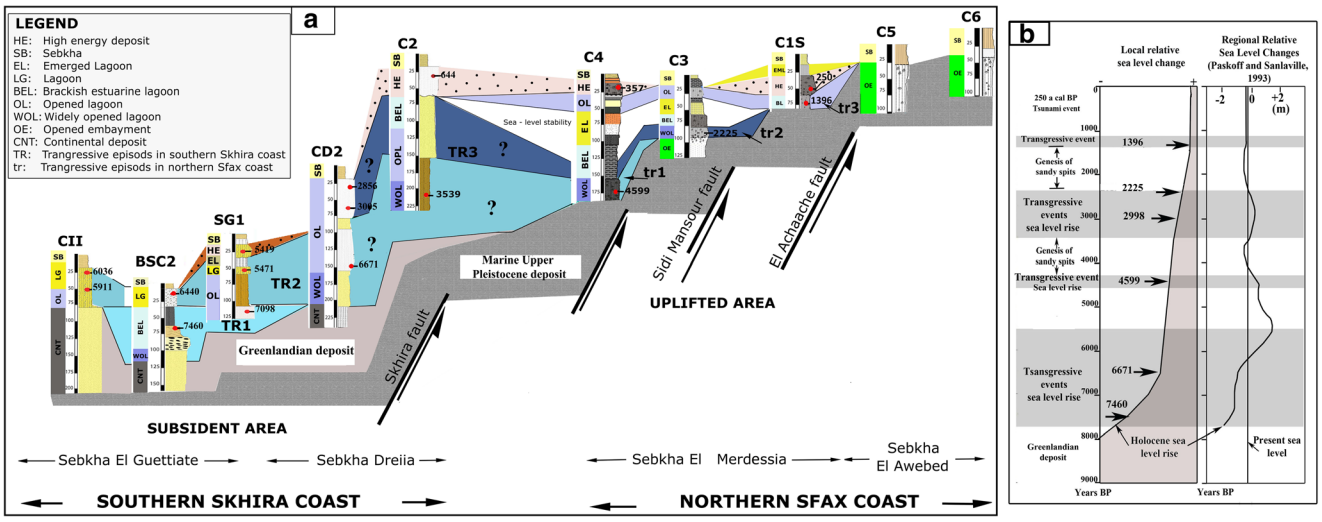

Fig. 14 **a** Correlation between the stratigraphy of northern Sfax coast (El Merdessia and El Awebed sebkhas) and southern Skhira coast (Dreiia and El Guettiate sebkhas). Transgressive episode (tr1 to tr3 and TR1 to TR3), period of sea-level stability, and high-energy events recognized in each coast. **b** Local and regional sea-level changes. Period of transgressions and of sandy spits genesis. Calibrated median ages for northern Sfax coast and southern Skhira coast

Ouda et al. (1998) identified, in Maknassy basin, a humid phase between 4 and 2 ka BP. In northern Tunisia (Medjerda region), Faust et al. (2004) recognized a wet period toward 2550 cal BP. In Moroccan Middle Atlas, high lake levels were achieved at about 2300 cal BP, related probably to the wetter Iberian and Roman periods in the northern Mediterranean (Damnati et al. 2016).

Period of relative sea-level stability and development of sand spit between 2225 and 1396 years cal BP

After the second transgression, the brackish ostracods and lagoonal mollusks are richer in C3 core and reveal the low values of species number and of diversity index (*H* and *E*) and the high density. Subsequently, they disappear. This evolution reflects the settlement of a brackish lagoon, evolving to the closure (CL) and emersion. The brackish lagoon is also argued, in the area of C4 core, by the presence of the dominant *L. elliptica*, preferring higher hydrodynamic conditions and estuarine environments, associated to *C. torosa* in C4 core and by the impoverishment of the coastal and marine taxa. *C. torosa* which reaches up to 100% indicates the diminution of environment energy and proved by the high percentage (80%) of the fine fraction (< 125 μm). The reduced marine influence was probably caused by the formation of sand barriers, closing off the estuarine lagoons from direct communication with the ocean. Such barriers, which isolate the lagoon from the open sea, control lagoon dynamics and water salinity. In addition, this period favored the deposition of quartz grains eroded from the watershed on the coast. Furthermore, the erosion of Upper Pleistocene sands from the coastline outcrops by means of alongshore drift currents, enriched even more the environment in quartz grains. These latter are subjected to the action of the drift currents, responsible for the buildup of sand barrier spits. Intense weathering, high erosion rates in the adjacent watershed, and fluvial transport promoted the dilution of marine waters and the development of brackish and estuarine ostracod and lagoonal mollusks and the disappearance of marine micro- and macrofauna.

The genesis of littoral bars, resulting in the closure of lagoons, was mentioned in studies along the Gulf of Gabes in several sites, such as Dreiia sebkha from 6671 years cal BP (Zaïbi et al. 2016), Aouled Ridha sebkha (Gargouri 2009), Bin El Oudiane lagoon toward 5.0 ka cal BP (Masmoudi et al. 2005), and Boujmel sebkha between 6.8 and 4.0 ka cal BP (Lakhdar et al. 2006). The action of drift currents was also mentioned at Botria lagoon by Trousset (1992), at Chebba sebkha by Zaïbi et al. (2006), and at Rass Dimas by Amrouni (2008) where it was responsible for a strong coastal accretion during historic times. Indeed, these currents affected the historic harbors, civilizations, and the genesis of lagoonal environments.

The third marine transgression (tr3), toward 1396 years cal BP

In C1 core, the diversification of ostracod assemblages with the appearance of marine and coastal taxa, associated with the increase of species number and the reduction of density, suggests the settlement of open marine conditions, following a marine transgression toward 1396 years cal BP. This transgression (tr3) is also recorded in C3 and C4 cores and not in C5 and C6 core of El Awebed sebkha, which always remained emerged. In C3 core (U6), tr3 is evidenced by the reappearance of the brackish, lagoonal, and coastal ostracods and the high values of the biocenotic parameters and diversity indices *H* and *E*. In C4 core, tr3 reveals the recurrence of marine and coastal ostracods and lagoonal mollusks after the episode of closure (CL) and the increase of the ostracod species richness and density.

During the same period, data inferred from archeological sites of Punic–Roman age, located along the coast of Tunisia, all aged between 2 and 1.5 ka BP, indicate that local relative sea level increased 0.2 to 0.5 m since the last 2 ka BP (Anzidei et al. 2011). In addition, Gargouri et al. (2007) identified, based on a sedimentological study, a marine transgression toward 1900 years BP in Gargour coast (southern Sfax). This interval also registers a dry period described by Brun (1992) who denotes arid vegetation between 1.5 and 1.0 ka cal BP by means of marine pollen profiles (Gulf of Gabes). In addition, Stevenson et al. (1993) identified in subsurface sediment of Ichkeul Lake (northern Tunisia) the development of saline microfauna from 1.4 ka cal BP. Likewise, Hunt et al. (2001) assume a steppe landscape in western Libya that persisted until the early Arab period. According to Rohdenburg (1977), a phase of geomorphodynamic stability is indicated in Morocco from 2100 to 2000 years cal BP.

Tsunami extreme event toward 250 years cal BP

The changes in sediment composition for the deposition of sands, organized in fining upward with erosional base highlighted by Upper Pleistocene lithoclasts, bioclasts, pottery fragments, and charcoal particles, in unit U2, C1S core and unit U5, C4 core, indicate a high energetic environment with a sufficient flow velocity. The ostracod associations show marine, coastal, and lagoonal taxa associated to brackish dominant species with mud preferences and a prevalence of eurytherm as well as euryhaline taxa. The dominance of *C. torosa* taxa suggests a sheltered brackish environment with rapid sand accumulation. In addition, the abrupt enrichment of coastal and marine ostracods, the highest values of species number and density of ostracofauna and mollusks, and the presence of allochthonous taxa point out a tsunami event. In Henchir El Mejdoul cliff, this peculiar event is evidenced by (i) the locally extensive deposits up to 160 m inland rising in

altitude of about 0.75 m, (ii) the rework of Holocene microfauna and Upper Pleistocene sands rich in mollusks eroded from the marine substratum, (iii) the high concentration of poorly stratified and poorly sorted shells, (iv) the dominance of articulated bivalves and sharpened shells, and (v) the percentage of broken and abraded mollusks (70%) and the abnormal ratio between juvenile and adult ostracod taxa (Khadraoui et al. 2018). In fact, Bahrouni et al. (2013) indicate that the Villafranchian crust and the Upper Pleistocene marine carbonates outcropping in the Tunisian coast are affected by both major and minor fault trending N–S and E–W, creating tilted blocks. The most active ones are responsible for the displacements of the Upper Pleistocene marine carbonates (> 500 m). In addition, historical deformations, as well as recent seismic events of moderate magnitude, were clearly observed in several localities of the Gulf of Gabes and Sfax-Agareb area. On the other hand, Roman then Arabic historic sources indicated strong seismic activities, with numerous devastating earthquakes, such as in Utique (410 AD), Kairouan (854 AD), and Tunis (856 AD) (INM Catalog). Also, Ambraseys (1962) reported a strong earthquake in Sfax at 1750 AD corresponding, probably, to the reactivation of the Henchir El Mejdoul faults.

This extreme high-energy event is not new in Tunisia; indeed, several authors mentioned paleotsunami deposits such as (i) Wood (1994), who interpreted the Upper Pleistocene boulder beds on Hergla and Chebba coasts as results of tsunami or severe storm surge during substage 5e; (ii) May et al. (2010) recognized, for the first time, boulders, on the coast of Haouaria (Cap Bon), whose characteristics point out to a tsunami-induced transport rather than a storm-induced dislocation; and (iii) Frébourg et al. (2010) were the first authors who indicate the possibility of a prehistoric tsunami deposit, 8 ka BP in age, found within Sidi Salem eolianites in Jerba island coast. It is to highlight that during the eighteenth century, several tsunamis occurred, between 1700 and 1775 AD, in Mediterranean coasts such as in Italy (Mastronuzzi and Sanso 2004), Spain (Kelletat et al. 2005), Algeria (Maouche et al. 2005; Papadopoulos 2009), and in Portugal coast (Quintela et al. 2016). Also, Tinti et al. (2005) describe the most devastating Italian tsunami which hit eastern Sicily and the Messina straits at 1908 and mention that the east Tunisian coast was highly prone to a 1908 scenario based on their numerical simulation. So, the extreme event recognized at Sfax northern coast can be related to the mega tsunami, triggered by the 1908 AD earthquakes of eastern Sicily. It can be correlated to the upper unit of core C2 that was interpreted by Zaïbi et al. (2016) as a possible washover deposit (Fig. 14). The comparison between the mentioned criteria of C2 core (abundance of bivalve fragments, high-energy shifting substrate, charcoal, pottery fragments, coarser sediments, and mixture of ostracod associations) and those herein mentioned allows this correlation.

Conclusion

Based on a multiproxy approach, analyzing paleontological, sedimentological, and radiochronological data from five sediment cores, we produced a reconstruction of the Holocene evolution of the two sebkhas El Merdessia and El Awebed of the northern Sfax coast and compared this evolution to the Skhira coast. In the early Holocene, the sea level rose at approximately 7460 and 6671 years cal BP and marine conditions reached the south Skhira coast, filling this area with sand and silts. These two transgressional events have no counterpart in northern Sfax coast, which in the sebkha El Merdessia recorded the following: (i) three transgressive phases toward 4599, 2225, and 1396 years cal BP, allowing the settlement of a widely opened lagoon, evidenced by the high values of ostracod species richness, the importance of lithoclasts, and the diversity of ostracod and mollusk associations; (ii) between 2225 and 1396 years BP, a period of relative sea-level stability and development of drift current which authorized the buildup of sandy spits and the genesis of a closed lagoon; (iii) the last transgressive event (1396 years cal BP in age) was responsible for the settlement of an open lagoon which allowed the diversification of ostracod assemblages, with the dominance of marine taxa; and (iv) the changes in ostracod and mollusk associations, the abnormal population structure, and the presence of reworked continental materials, such as pottery fragments, lithoclasts, and charcoal particles in coarse sands, point to a high-energy tsunami event toward 250 years cal BP. The El Awebed sebkha, which records the MIS 5.5 by means of the sedimentation of quartz grains rich in warm fossils such as *P. latus* and *C. mediterraneus* associated to *Loripes* sp., *Cerastoderma glaucum*, and *Cerithium vulgatum*, remains emerged during the Holocene time. The activity of the faults visible in Sfax coast seems to be responsible of the time shift of the sedimentation between the two sebkhas El Awebed and El Merdessia. On a larger scale, the comparison of the behavior of Sfax and Skhira coasts highlights the influence of the neotectonic and the role played by the replay of faults during Holocene sedimentation. A time shift of sedimentation is due to the uplift of Sfax northern coast unlike the southern Skhira subsidence.

Acknowledgments The authors are thankful to the editor Dr. Karin Bryan for the constructive collaboration and prompt response. We equally acknowledge the efforts of the anonymous reviewers and their fruitful comments and objective assessment of the manuscript. The contribution of Prof. Martin Langer (Bonn University) in Foraminifera determination, Prof. Kamel Zouari in radiometric analyses, and Kamel Maaloul in language polishing and proofreading services are highly appreciated.

References

Abrantes F, Lebreiro S, Rodrigues T, Gil I, Bartels-Jonsdottir H, Oliveira P, Kissel C, Grimalt JO (2005) Shallow-marine sediment cores record climate variability and earthquake activity off Lisbon (Portugal) for the last 2000 years. Quat Sci Rev 24:2477–2494

Ambraseys NN (1962) The seismicity of Tunis. Ann Geophys 15:233–244

Amrouni O (2008) Morphodynamique d'une plage sableuse microtidale à barres: côte nord de Mahdia (Tunisie orientale). Thèse de Doctorat en Sciences géologiques, Faculté des Sciences de Tunis. 296 p

Anzidei M, Antonioli F, Lambeck K, Benini A, Soussi M, Lakhdar R (2011) New insights on the relative sea level change during Holocene along the coasts of Tunisia and western Libya from archaeological and geomorphological markers. Quat Int 232:5–12

Athersuch J, Horne DJ, Whittake JE (1989) Marine and brackish water ostracods (super families Cypridacea and Cytheracea): keys and notes for the identification of the species. Synopses of the British fauna (new series) 43. E. J. Brill, Leiden 7, 345 pp

Bahrouni N, Bouaziz S, Soumaya A, Ben Ayed N, Attafi K, Houla Y, El Ghali A, Rebai N (2013) Active deformation analysis and evaluation of earthquake hazard in Gafsa region (Southern Atlas of Tunisia). J Seismol 18:235–256

Baumann J, Chaumillon E, Schneider JL, Jorissen F, Sauriau PG, Richard P, Bonnin J, Schmidt S (2017) Contrasting sediment records of marine submersion events related to wave exposure, southwest France. Sediment Geol 353:158–170

Ben Hamad A, Viehberg F, Khadraoui A, Zaïbi C, Trabelsi Y, Mouanga G, Langer M, Abida H, Kamoun F (2018) Water level and atmospheric humidity history of Lake Ichkeul (northern Tunisia) during the last 3000 years. Arab J Geo Sci 11:316

Benzécri JP (1980) Pratique de l'analyse des données. Editions Dunod, Paris

Bernabéu-Puga A, Aguirre J (2017) Contrasting storm- versus tsunami-related shell beds in shallow-water ramps. Palaeogeogr Palaeoclimatol Palaeoecol 471:1–14

Bonaduce G, Ciampo G, Masoli M (1975) Distribution of Ostracoda in the Adriatic Sea. Reprinted from the Pubb. Staz Zoo Napoli 40:1–304

Boomer I, Eisenhauer G (2002) Ostracod faunas as palaeoenvironmental indicators in marginal marine environments. In: Holmes J, Chivas A. (eds) The Ostracoda: applications in Quaternary research. Geophys Mono 131:135–149

Boomer I, Whatley R (1992) Ostracoda and dysaerobia in the Lower Jurassic of Wales: the reconstruction of past oxygen levels. Palaeogeogr Palaeoclimatol Palaeoecol 99:373 379

Bouchet P, Rocroi JP (2005) Classification and nomenclator of gastropod families. Malacol Instit Malacol 47:1–397

Bouchet P, Rocroi JP (2010) Nomenclator of bivalve families with a classification of bivalve families. Malacol Instit Malacol 52:1–184

Brun A (1992) Pollens dans les séries marines du Golfe de Gabès et du plateau des Kerkennah (Tunisie): signaux climatiques et anthropiques. Quaternaire 3:31–39

Brun A, Rouvillois-Brigol M (1985) Apport de la palynologie à l'histoire du peuplement en Tunisie. In Palynologie Archéologique, Notes et monographies technique 17:213–226

Carbonel P (1980). Les ostracodes et leur intérêt dans la définition des écosystèmes estuariens et de plateforme continentale. Essais d'application à des domaines anciens. Mémoire de l'Institut de Géologie du Bassin d'Aquitaine 11, pp. 350

Carbonel P (1982) Les Ostracodes, traceurs des variations hydrologiques dans les systèmes de transition eau douce-eau salée. Mém Soc Géol Fr 144:117–128

Carbonel P (1988) Ostracods and the transition between fresh and saline waters. In: De Deckker P, Colin J-P, Peypouquet JP (eds) Ostracoda in the earth sciences. Elsevier, Amsterdam, pp 157–173

Carbonel P, Jouanneau JM (1982) The evolution of a coastal lagoon system: hydrodynamics determined by ostracofauna and sediments—the Bonne-Anse Bay (Pointe de la Coubre, France). Geo-Mar Lett 2:65–70

Carbonel P, Pujos M (1981) Comportement des microfaunes benthiques en milieu lagunaire. Actes du Premier Congrès National des Sciences de la Terre, Tunis, pp 127–139

Damnati B, Etebaai I, Benjilani H, El Khoudri K, Reddad K, Taieb M (2016) Sedimentology and geochemistry of lacustrine terraces of three Middle Atlas lakes: paleohydrological changes for the last 2300 cal BP in Morocco (western Mediterranean region). Quat Int 404:163–173

Delibrias G (1985) Le carbone 14. In: Roth E, Poty B (eds) Méthodes de datation par les phénomènes nucléaires naturels. Application. ÉditionsMasson, Paris, pp 421–458

Despois J (1955) La Tunisie orientale sahel et basse steppe. Publication de l'institut des hautes études de Tunis section des lettres, I. 552 p

Donato SV, Reinhardt EG, Boyce JI, Rothaus R, Vosmer T (2008) Identifying tsunami deposits using bivalve shell taphonomy. Geol 36:199–202

Engel M, Oetjen J, May SM, Brückner H (2016) Tsunami deposits of the Caribbean—towards an improved coastal hazard assessment. Ear-Sci Rev 163:260–296

Fatela F, Taborda R (2002) Confidence limits of species proportions in microfossil assemblages. Mar Micropaleontol 45:169–174

Faust D, Zielhofer C, Escudero RB, Diaz delolmo F (2004) High-resolution fluvial record of late Holocene geomorphic change in northern Tunisia: climatic or human impact? Quat Sci Rev 23: 1757–1775

Frébourg G, Hasler CA, Davaud E (2010) Catastrophic event recorded among Holocene eolianites (Sidi Salem Formation, SE Tunisia). Sed Geol 224:38–48

Frenzel P, Wrozyna C, Xie M, Zhu L, Schwalb A (2010) Palaeo-water depth estimation for a 600-year record from Nam Co (Tibet) using an ostracod-based transfer function. Quat Int 218:157–165

Gargouri D (2009) Etude géomorphologique, sédimentologique et géochimique de la frange littorale de Sfax à la Skhira: Apport à l'aménagement côtier. Thèse de doctorat université de Sfax 207 p

Gargouri D, Zaïbi C, Kamoun F, Jedoui Y, Montacer M (2007) Etude morphologique comparative entre les flèches de Chaffar et la flèche de Ras Kabboudia (Sfax, cote orientale de la Tunisie). Notes Serv Géol Tunis 75:105–119

Goy JL, Zazo C, Dabrio CJ, Lario J, Borja F, Sierro FJ, Flores JA (1996) Global and regional factors controlling changes of coastlines in southern Iberia (Spain) during the Holocene. Quat Sci Rev 15: 773–780

Hammer Ø, Harper DAT, Ryan PD (2001) Past: paleontological statistics software package for education and data analysis. Palaeontol Electron 4(1):9

Hindson RA, Andrade C, Dawson AG (1996) Sedimentary processes associated with the tsunami generated by the 1755 Lisbon Earthquake on the Algarve Coast, Portugal. Phys Chem Earth 21: 57-63

Hindson RA, Andrade C (1998) Sedimentation and hydrodynamic processes associated with the tsunami generated by the 1755 Lisbon earthquake. Quat Int 56:27–38

Houla Y, Bahrouni N, Fakhraoui M (2013) Geological map of Tunisia, Sidi Salah. Editions of Geol Surv Nat Off of Mines, Tunisia

Hunt CO, Rushworth G, Gilbertson DD, Mattingly DJ (2001) Romano-Libyan dry land animal husbandry and landscape: pollen and palynofacies analyses of coprolites from a farm in the Wadi el-Amud, Tripolitania. J Archaeol Sci 28:351–363

Jedoui Y (2000) Sédimentologie et géochronologie des dépôts littoraux quaternaires: reconstitution des variations des paléoclimats et du niveau marin dans le Sud-est tunisien. Doctoral dissertation, University of Tunis II, 338 pp

Kelletat D, Whelan F, Bartel P, Scheffers A (2005) New tsunami evidences in southern Spain-Cabo de Trafalgar and Mallorca Island. In: Sanjaume E, Matheu JF (eds) GeomorfologiaLitoral I

Quarternari, Homenatge al professor Vincenç M. RosselloI Verger. University of Valencia, Valencia, pp 215–222

Khadraoui A, Kamoun M, Ben Hamad A, Zaïbi C, Bonnin J, Viehberg F, Bahrouni N, Sghari A, Abida H, Kamoun F (2018) New insights from microfauna associations characterizing palaeoenvironments, sea level fluctuations and a tsunami event along Sfax Northern Coast (Gulf of Gabes, Tunisia) during the Late Pleistocene-Holocene. J Afr Earth Sci 147:411–429

Lachenal AM (1989) Écologie des Ostracodes du domaine application au Golfe de Gabès (Tunisie Orientale). Les variations du niveau marin depuis 30.000 ans. Doc Lab Géol Lyon 108:1–239

Lakhdar R, Soussi M, Ben Ismail MH, M'Rabet A (2006) A Mediterranean Holocene restricted coastal lagoon under arid climate: case of the sedimentary record of Sabkha Boujmel (SE Tunisia). Palaeogeogr Palaeoclimatol Palaeoecol 241:177–191

Lambeck K, Yokoyama Y, Purcell T (2002) Into and out of the Last Glacial Maximum: sea-level change during oxygen isotope stages 3 and 2. Quat Sci Rev 21:343–360

Laprida C (2001) Les ostracodes traceurs de conditions hydrologiques à petite échelle: exemple d'interprétation dans l'Holocène. Geobios 34:707–720

Mansouri-Menaouar R, Carbonel P (1980) Les déplacements d'ostracodes et leurs relations avec les courants dans la lagune de Ghar el Melh. Bull Soc Sci Nat Tunisie 16:55–55

Mansouri-Menaouar R, Carbonel P, Bobier C (1979) A propos de l'évolution récente de la sebkha de l'Ariana (Tunisie). Bull Off Nat Pêches Tunisie 3:157–163

Maouche S, Morhange C, Meghraoui M (2005) Large boulder accumulation on the Algerian coast evidence tsunami events in the western. Med Mar Geol 262:96–104

Masmoudi S, Yaich C, Ammoun M (2005) Evolution et morphodynamique des iles barrières et des flèches littorales associées à des embouchures microtidales dans le Sud- Est tunisien. Bull Inst Sci Sec Sc Terre 27:65–81

Mastronuzzi G, Sanso P (2004) Large boulder accumulations by extreme waves along the Adriatic coast of southern Apulia (Italy). Quat Int 120:173–184

Mauz B, Elmejdoub N, Nathan R, Jedoui Y (2009) Last interglacialcoastalenvironments in the Mediterranean–Saharan transition zone. Palaeogeogr Palaeoclimatol Palaeoecol 279:137–146

May SM, Willershäuser T, Vött A (2010) Boulder transport by high-energy wave events at Cap Bon (NE Tunisia). Coast Rep 16:1–10

Milker Y, Schmiedl G, Betzler C, Andersen N, Theodor M (2012) Response of Mallorca shelf ecosystems to an early Holocene humid phase. Mar Micropaleontol 90-91:1–12

Morzadek-Kerfourn MT (2002) L'évolution des Sebkhas du golf de Gabès (Tunisie) à la transition Pléistocène supérieur-Holocène. Quaternaire 13:111–123

Nachite D, Rodríguez-Lázaro J, Martín-Rubio M, Pascual A, Bekkali B (2013) Distribution and ecology of recent ostracods from the Tahadart estuary (NW Morocco). Rev Micropaleontol 53:3–15

Oh JK, Carbonel P (1978) Les ostracodes du delta de l'Eyre: répartition au cours de l'année 1977. Bull InstGéol Bassin d'Aquitaine 24:125–130

Ouda B, Zouari K, Ben Ouezdou H, Chkir N, Causse C (1998) Nouvelles données paléoenvironnementales pour le Quaternaire récent en Tunisie centrale (basin de Maknessy). Earth Planet Sci 326:855–886

Padmanabha B, Belagali SL (2008) Ostracods as indicators of pollution in the lakes of Mysore. J Environ Biol 29:711–714

Papadopoulos GA (2009) Tsunamis, chapter 17. In: Woodward J (ed) Physical geography of the Mediterranean. Oxford University Press, Oxford, pp 493–512

Pascual A, Carbonel P (1992) Distribution and annual variations of *Loxoconcha elliptica* in the Gernika estuary (Bay of Biscay). Geobios 25:495–503

Paskoff R, Sanlaville P (1983) Les côtes de la Tunisie: variation du niveau marin depuis le Tyrrhénien. Maison de l'orient, Lyon, p 192

Perthuisot JP (1975) La Sabkha El Melah de Zarzis: genèse et évolution d'un bassin paralique. Trav Lab Géol E.N.S Paris 9:252

Peypouquet JP, Carbonel P, Ducasse M, Tölderer-Farmer M, Lété C (1988) Environmentallycuedpolymorphism of ostracods. In: Hanai T, Ikeya N, Ishizaki K (eds) Evolutionary biology of Ostracoda—its fundamentals and applications. Kodansha, Tokyo, pp 1003–1018

Pielou EC (1966) The measurement of diversity in different types of biological collections. J Theor Biol 13:131–144

Quintela M, Costa PJM, Fatela F, Drago T, Hoska N, Andrade C, Freitas MC (2016) The AD 1755 tsunami deposits onshore and offshore of Algarve (south Portugal): sediment transport interpretations based on the study of Foraminifera assemblages. Quat Inter 408:123–138

Reimer PJ, Bard E, Bayliss A, J Warren Beck JW, Blackwell PG, Bronk Ramsey CB, Buck CE, Cheng H, Edwards RL, Friedrich M, Grootes PM, Guilderson PT, Haflidason H, Hajdas I, Hatté C, Heaton TJ, Hoffmann DL, Hogg AG, Hughen KA, Kaiser KF, Kromer B, Manning SW, Niu M, Reimer RW, Richards DA, Scott EM, Southon JR, Staff RA, Turney CSM, Van der Plicht J (2013) IntCal13 and Marine13 radiocarbon age calibration curves, 0-50000 years cal BP. Radiocarbon 4:1869–1887

Reinhardt EG, Goodman BE, Boyce JI, Lopez G, van Hengstum P, Rink W, Mart Y, Raban A (2006) The tsunami of 13 December A.D. 115 and the destruction of Herod the Great's harbor at Caesarea Maritima, Israel. Geology 34:1061–1064

Richmond B, Szczuciński W, Chagué-Goff C, Goto K, Sugawara D, Witter R, Tappin DR, Jaffe B, Fujino S, Nishimura Y, Goff J (2012) Erosion, deposition and landscape change on the Sendai coastal plain, Japan, resulting from the March 11, 2011 Tohoku-oki tsunami. Sed Geol 282:27–39

Rohdenburg H (1977) Neue 14C-Daten ausMarokko und Spanien und ihreAussagenfür die ReliefundBodenentwicklungimHolozän und Jungpleistozän. Catena 4:215–228

Ruiz F, Rodríguez-Ramírez A, Cáceres LM, Rodríguez Vidal J, Carretero MI, Abad M, Olías M, Pozo M (2005) Evidence of high-energy events in the geological record: mid-Holocene evolution of the southwestern Doñana National Park (SW Spain). Palaeogeogr Palaeoclimatol Palaeoecol 229:212–229

Ruiz F, Abad M, Galán EI, González I, Aguilá I, Olías M, Gómez Ariza JL, Cantano M (2006) The present environmental scenario of El Melah Lagoon (NE Tunisia) and its evolution to a future sabkha. J Afr Earth Sci 44:289–302

Ruiz F, Borrego J, López-González N, Abad M, Gonzlez-Regalado ML, Carro B, Pendón JG, Rodríguez-Vidal J, Cáceres LM, Prud ncio MI, Dias MI (2007) The geological record of a mid-Holocene marine storm in southwestern Spain. Geobios 40:689–699

Siani G, Paterne M, Arnold M, Bard E, Metivier B, Tisnerat N, Bassinot F (2000) Radiocarbon reservoir ages in the Mediterranean Sea and Black Sea. Radiocarbon 42:271–280

Siani G, Paterne M, Michel E, Sulpizio R, Sbrana A, Arnold M, Haddad G (2001) Mediterranean Sea surface radiocarbon reservoir age changes since the Last Glacial Maximum. Science 294:1917–1920

Stevenson AC, Phethean SJ, Robinson JE (1993) Thepalaeosalinity and vegetational history of Garaet el Ichkeul, northwest Tunisia. Holocene 3:201–210

Stuiver M, Reimer PJ (1993) Extended 14C data base and revised CALIB 3.0 14C age calibration program. Radiocarbon 35:215–230

Tinti S, Armigliato A, Pagnoni G, Zaniboni F (2005) Scenarios of giant tsunamis of tectonic origin in the Mediterranean. ISET J Earth 42: 171–188

Trog C, Dana H, Frenzel P, Camacho S, Schneider H, Mäusbache R (2013) A multi-proxy reconstruction and comparison of Holocene palaeoenvironmental changes in the Alvor and Alcantarilha estuaries (southern Portugal). Rev Micropaleontol 56:131–158

Trousset P (1992) La vie littorale et les ports dans la Petite Syrte à l'époque romaine, dans Ve Coll. sur l'Histoire et l'Archéologie de l'Afrique du Nord (Avignon avril 1990). CTHS, Paris, pp 317–332

Vella C, Provansal M (2000) Relative sea-level rise and neotectonic events during the last 6500 a on the southern eastern Rhône delta, France. Mar Geol 170:27–39

Viehberg F, Frenzel P, Gosta H (2008) Succession of late Pleistocene and Holocene ostracode assemblages in a transgressive environment: a study at a coastal locality of the southern Baltic Sea (Germany). Palaeogeogr Palaeoclimatol Palaeoecol 264:318–329

Wood PB (1994) Optically stimulated luminescence dating of a late quaternary shoreline deposit, Tunisia. Quat Sci Rev 13:513–516

Zaïbi C, Kamoun F, Gargouri D, Jedoui Y, Montacer M (2006) Impact de la genèse et de l'évolution de la flèche sableuse de Rass Kaboudia sur les environnements littoraux de la région de Chebba (Tunisie). Apport des foraminifères benthiques et des mollusques. Notes du Service Géologique. Off Nat des Mines, Tunisie 74:93–106

Zaïbi C, Carbonel P, Kamoun F, Azri C, Kharroubi A, Kallel N, Jedoui Y, Montacer M, Fontugne M (2011) Evolution du trait de côte à l'Holocène supérieur dans la sebkha El-Guettiate de Skhira (Golfe de Gabès, Tunisie) à travers sa faune d'ostracodes et des foraminifères. Geobios 44:101–115

Zaïbi C, Carbonel P, Kamoun F, Fontugne M, Azri C, Jedoui Y, Montacer M (2012) Evolution of the sebkha Dreîaa (South-Eastern Tunisia, Gulf of Gabes) during the late Holocene: response of ostracod assemblages. Rev Micropaleontol 55:83–97

Zaïbi C, Kamoun F, Viehberg F, Carbonel P, Jedoui Y, Abida H, Fontugny M (2016) Impact of relative sea level and extreme climate events on the Southern Skhira coastline (Gulf of Gabes, Tunisia) during Holocene times: Ostracodes and foraminifera associations response. J Afr Earth Sci 118:120–136

Zazo C, Dabrio CJ, Goy JL, Lario J, Cabero A, Silva PG, Bardaji T, Mercier N, Borja F, Roquero E (2008) The coastal archives of the last 15 ka in the Atlantic-Mediterranean Spanish linkage area: sea level and climate changes. Quat Int 181:72–87

Publisher's note Springer Nature remains neutral with regard to jurisdictional claims in published maps and institutional affiliations.